CoA Note No. 67

THE COLLEGE OF AERONAUTICS
CRANFIELD

VORTEX TUBE PERFORMANCE DATA SHEETS

by

R. Westley

COLLEGE NOTE NO.67

JULY, 1957

THE COLLEGE OF AERONAUTICS

CRANFIELD

Vortex Tube Performance Data Sheets

-by-

R. Westley, D.C.Ae.

---

1. Introduction

Experiments to determine the effect of various operating and design parameters on the performance of a vortex tube are described in College of Aeronautics Note No. 30. The present note gives additional performance data on this tube and should be used as a supplement to Note No.30.

These data sheets are intended as an aid to the estimation of the performance of vortex tubes and to the design of vortex tubes with given characteristics. In particular, the present note provides the optimum values of the vortex tube parameters which give maximum temperature drops.

Figures 12-53 give temperature drop and cold mass flow ratio characteristics, figures 54-61 give the cold mass flow ratios at maximum temperature drop whilst figures 62-65 give the optimum inlet and cold outlet sizes for maximum temperature drop.

Prepared under Ministry of Supply Contract 7/Exptl/565/R3

2. NOTATION

p_i	inlet pressure
p_c	cold outlet pressure
p_h	hot outlet pressure
Δp_i	pressure differential across inlet flow meter
Δp_c	" " " cold " "
Δp_h	" " " hot " "
T_i	inlet temperature
T_c	cold "
T_h	hot "

$$\Delta T_c \equiv (T_i - T_c)$$

$$\left(\frac{\Delta T_c}{T_i}\right)_1 \equiv \frac{\Delta T_c}{T_i} \quad \text{for} \quad \frac{\partial \frac{\Delta T_c}{Ti}}{\partial \mu} = 0 \,.$$

$$\left(\frac{\Delta T_c}{T_i}\right)_2 \equiv \frac{\Delta T_c}{T_i} \quad \text{for} \quad \frac{\partial \frac{\Delta T_c}{T_i}}{\partial \mu} = 0, \quad \frac{\partial \left(\frac{\Delta T_c}{T_i}\right)_1}{\partial d_c} = 0.$$

$$\left(\frac{\Delta T_c}{T_i}\right)_3 \equiv \frac{\Delta T_c}{T_i} \quad \text{for} \quad \frac{\partial \frac{\Delta T_c}{T_i}}{\partial \mu} = 0, \quad \frac{\partial \left(\frac{\Delta T_c}{T_i}\right)_1}{\partial d_c} = 0, \quad \frac{\partial \left(\frac{\Delta T_c}{T_i}\right)_2}{\partial d_i} = 0.$$

$$\frac{T_c^*}{T_i} \equiv 1 - \left(\frac{\Delta T_c}{T_i}\right)_3$$

$$1 - \frac{\Delta T_{c\ \text{isentropic}}}{T_i} \equiv \left(\frac{p_c}{p_i}\right)^{\frac{\gamma-1}{\gamma}}, \quad \gamma = 1.40.$$

$$\Delta T_{c2} \equiv \left(\frac{\Delta T_c}{T_i}\right)_2 \times T_i \,.$$

$$\Delta T_{c3} \equiv \left(\frac{\Delta T_c}{T_i}\right)_3 \times T_i .$$

D diameter of vortex tube

d_c diameter of cold outlet

d_i equivalent inlet nozzle diameter $= \sqrt{\frac{4 \text{ Total inlet area}}{\pi}}$

ℓ_i length of inlet slot

$$\left(\frac{d_c}{D}\right)_1 \equiv \frac{d_c}{D} \text{ for } \frac{\partial\left(\frac{\Delta T_c}{T_i}\right)}{\partial\mu} = 0, \quad \frac{\partial\left(\frac{\Delta T_c}{T_i}\right)_1}{\partial\frac{d_c}{D}} = 0 .$$

$$\left(\frac{d_c}{D}\right)_2 \equiv \frac{d_c}{D} \text{ for } \frac{\partial\left(\frac{\Delta T_c}{T_i}\right)}{\partial\mu} = 0, \quad \frac{\partial\left(\frac{\Delta T_c}{T_c}\right)_1}{\partial\frac{d_c}{D}} = 0, \quad \frac{\partial\left(\frac{\Delta T_c}{T_i}\right)_2}{\partial\frac{d_i}{D}} = 0.$$

$$\left(\frac{d_i}{D}\right)_1 \equiv \frac{d_i}{D} \text{ for } \frac{\partial\left(\frac{\Delta T_c}{T_i}\right)}{\partial\mu} = 0, \quad \frac{\partial\left(\frac{\Delta T_c}{T_i}\right)_1}{\partial\frac{d_c}{D}} = 0, \quad \frac{\partial\left(\frac{T_c}{T_i}\right)_2}{\partial\frac{d_i}{D}} = 0.$$

R hot valve setting (revolutions)

$$\left(\frac{A_c}{A}\right)_2 \equiv \left\{\left(\frac{d_c}{D}\right)_2\right\}^2$$

$$\left(\frac{A_i}{A}\right)_1 \equiv \left\{\left(\frac{d_i}{D}\right)_1\right\}^2 .$$

μ cold mass flow ratio $= \frac{\text{cold mass flow}}{\text{inlet mass flow}}$

μ_1 cold mass flow ratio at $\frac{\Delta T_c}{T_i} = \left(\frac{\Delta T_c}{T_i}\right)_1$

μ_2 " " " " " " $= \left(\frac{\Delta T_c}{T_i}\right)_2$

μ_3 " " " " " " $= \left(\frac{\Delta T_c}{T_i}\right)_3$

3. LIST OF FIGURES & DATA SHEETS

Figs. 42-46. Variation of maximum temperature drop ratio $\left(\frac{\Delta T_c}{T_i}\right)_1$ with cold outlet diameter ratio $\left(d_c/D\right)$ for various pressure ratios $\left(p_i/p_c\right)$.

$\frac{d_i}{D}$ =	.266	.376	.461	.532	.595
—	Fig.42.	Fig.43.	Fig.44.	Fig.45.	Fig.46.

Fig. 47. Variation of temperature drop ratio $\left(\frac{\Delta T_c}{T_i}\right)_2$ with pressure ratio $\left(p_i/p_c\right)$ for optimum cold outlet diameter, optimum value setting and given inlet size $\left(\frac{d_i}{D}\right)$.

Fig. 48. Variation of temperature drop ratio with inlet size for optimum cold outlet and valve setting, $\left(\frac{p_i}{p_c} = 1.5, 2.0, 3.0, 4.0, 5.0, 6.0, 7.0\right)$.

$$\left(\frac{\Delta T_c}{T_i}\right)_2 \sim \frac{d_i}{D}$$

Fig. 49. Variation of temperature drop efficiency with pressure ratio at optimum cold outlet size, optimum valve setting and fixed inlet diameter.

$$\left(\frac{d_i}{D} = .266, .376, .461, .532, .595\right).$$

$$\frac{\Delta T_{c_2}}{\Delta T_{c\ ISEN}} \sim \frac{p_i}{p_c}.$$

Fig. 50. Variation of refrigeration efficiency with pressure ratio $\left(p_i/p_c\right)$ at optimum valve setting and cold outlet diameter for maximum temperature drop ratio $\left[\frac{\mu_2\left(\frac{\Delta T_c}{T_i}\right)_2}{\left(\frac{\Delta T_c}{T_i}\right)_{ISEN}}\right]$

Fig. 51. Variation of temperature drop ratio $\left(\frac{\Delta T_c}{T_i}\right)_3$ and refrigeration ratio $\left[\mu_3\left(\frac{\Delta T_c}{T_i}\right)_3\right]$ with pressure ratio at maximum temperature drop and optimum conditions.

Fig 52. Power law variation of temperature drop ratio and refrigeration ratio with pressure ratio $\left(p_i/p_c\right)$ at maximum temperature drop.

Fig. 53. Variation of temperature drop efficiency $\left[\left(\frac{\Delta T_c}{T_i}\right)_3 \Big/ \left(\frac{\Delta T_c}{T_i}\right)_{ISEN}\right]$ and refrigeration efficiency

$$\frac{\mu_3\left(\frac{\Delta T_c}{T_i}\right)_3}{\left(\frac{\Delta T_c}{T_i}\right)_{ISEN}}$$

with pressure ratio $\left(p_i/p_c\right)$ at maximum temperature drop.

Fig. 54-58. Variation of cold mass flow ratio (μ_1) with cold outlet diameter ratio $\left(d_c/D\right)$ at optimum valve setting

$\frac{d_i}{D}$ =	.266	.376	.461	.532	.595
	Fig.54.	Fig.55.	Fig.56.	Fig.57.	Fig.58.

Fig. 59. Variation of cold mass flow ratio (μ_2) with inlet diameter ratio $\left(d_i/D\right)$ at optimum valve setting and optimum cold outlet diameter.

Fig. 60. Variation of cold mass flow ratio (μ_2) with pressure ratio $\left(p_i/p_c\right)$ at optimum valve setting and optimum cold outlet diameter.

Fig. 61. Variation of cold mass flow ratio with pressure ratio for optimum valve setting, optimum cold outlet diameter and optimum inlet diameter

$$\dot{\mu}_3 \sim \frac{p_i}{p_c}$$

Fig. 62. Variation of optimum cold outlet diameter with inlet diameter $\left(\frac{p_i}{p_c} - 1.5, 2, 3, 4, 5, 6, 7\right)$.

$$\left(\frac{d_c}{D}\right)_1 \sim \frac{d_i}{D}$$

Fig. 63. Variation of optimum cold outlet diameter with pressure ratio for fixed inlet diameters, $\left(\frac{d_i}{D} = .266, .376, .461, .532 \; \& \; .595\right)$.

$$\left(\frac{d_c}{D}\right)_1 \sim \frac{p_i}{p_c}$$

Fig. 64. Optimum inlet and cold outlet diameters for maximum temperature drop.

$$\left(\frac{d_i}{D}\right)_1 \sim \frac{p_i}{p_c}$$

$$\left(\frac{d_c}{D}\right)_2 \sim \frac{p_i}{p_c}$$

Fig. 65. Optimum inlet and cold outlet areas for maximum temperature drop.

$$\left(\frac{A_i}{A}\right)_1 \sim \frac{p_i}{p_c}$$

$$\left(\frac{A_c}{A}\right)_2 \sim \frac{p_i}{p_c}$$

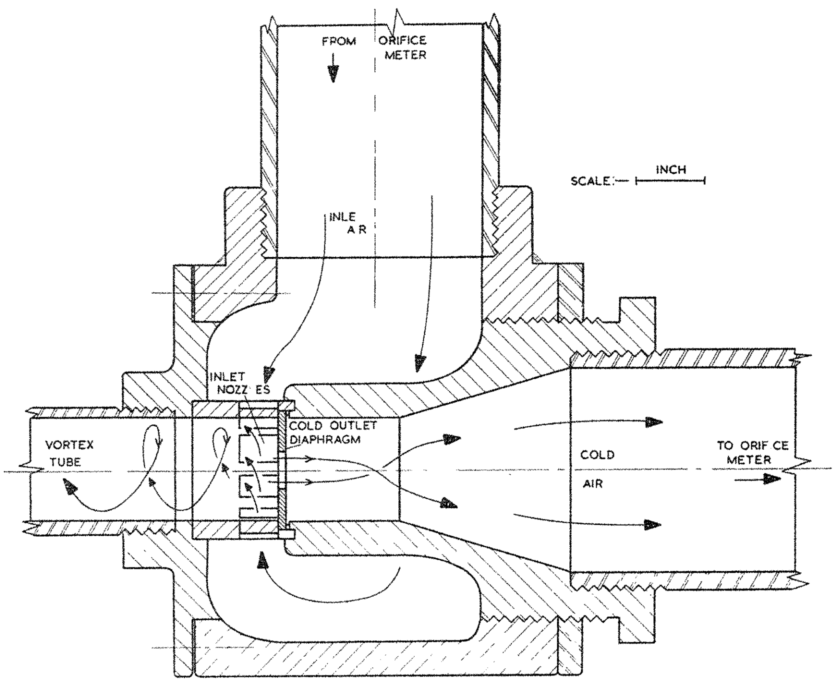

INLET CHAMBER AND COLD OUTLET

FIG. 1

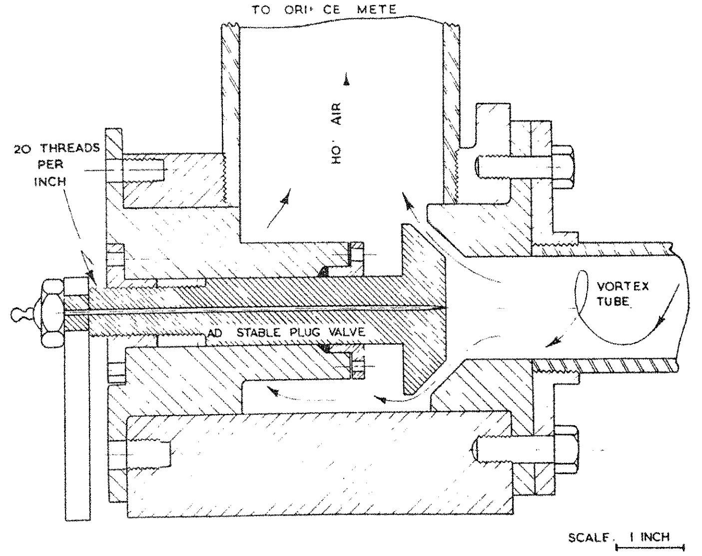

HOT AIR OUTLET VALVE

FIG. 2.

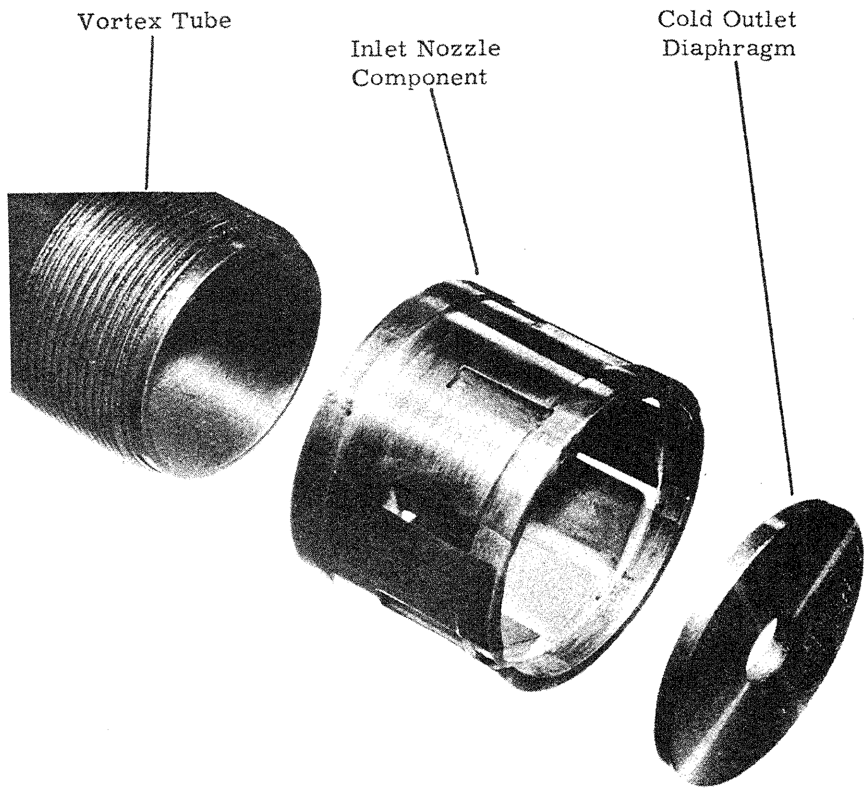

FIGURE 3. EXPLODED VIEW OF COLD OUTLET DIAPHRAGM,

INLET NOZZLE COMPONENT AND TUBE.

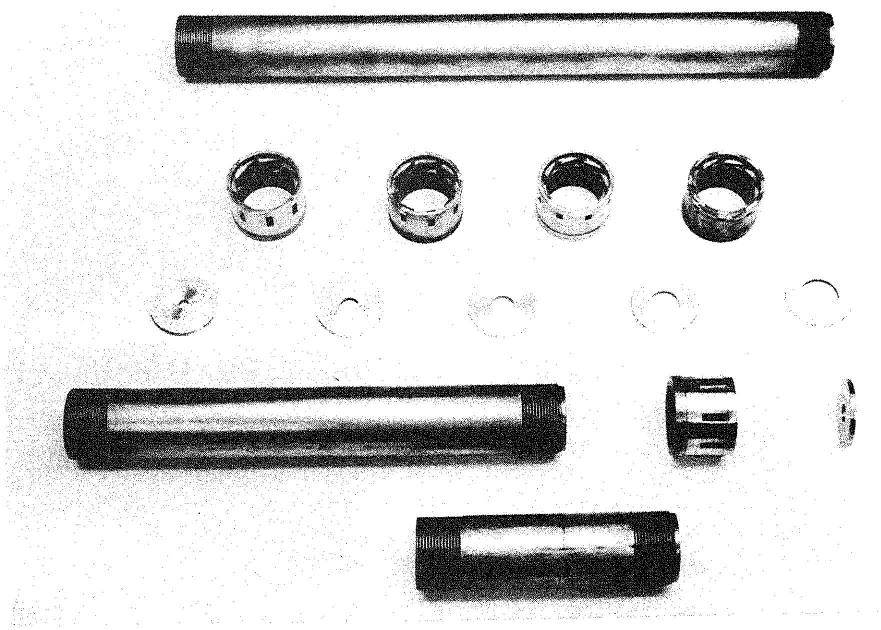

FIGURE 4 ALTERNATIVE VORTEX TUBE COMPONENTS

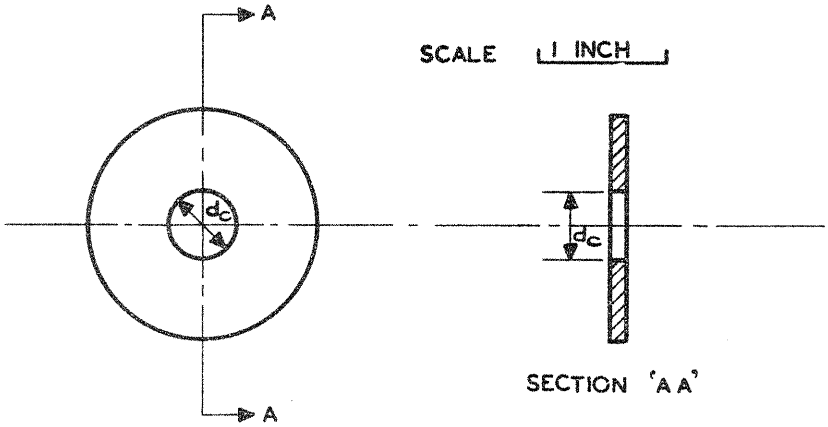

FIGURE 5. COLD OUTLET DIAPHRAGM

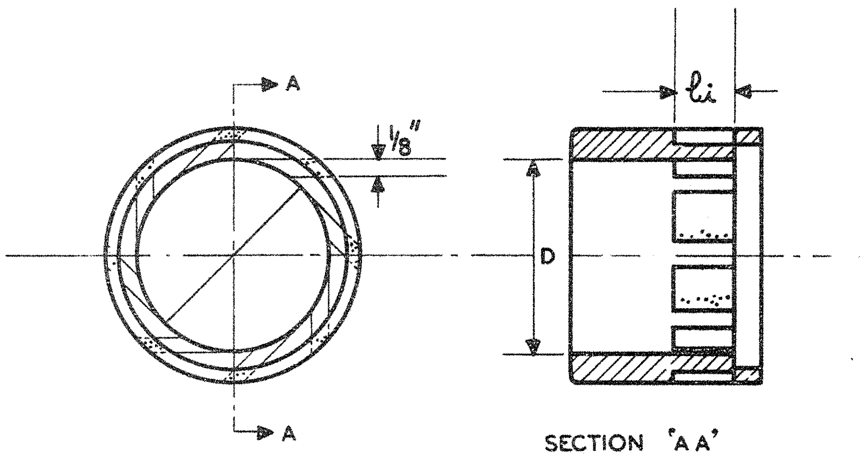

FIGURE 6. INLET NOZZLES

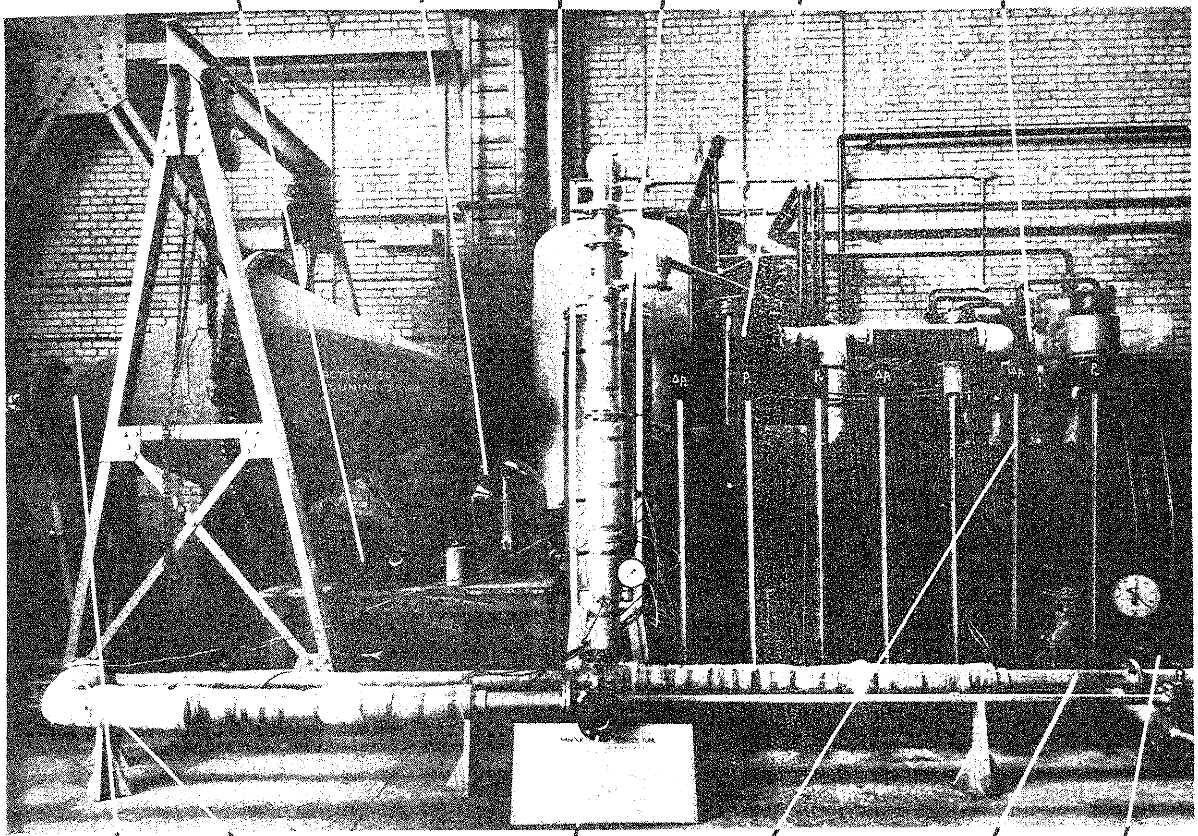

FIGURE 7. GENERAL VIEW OF VORTEX TUBE APPARATUS

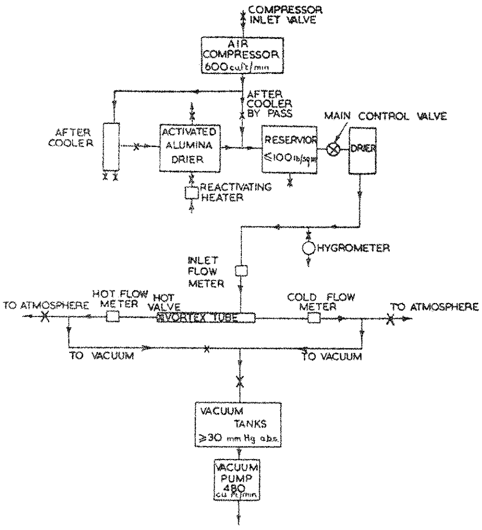

GENERAL LAYOUT OF VORTEX TUBE APPARATUS

FIG. 8.

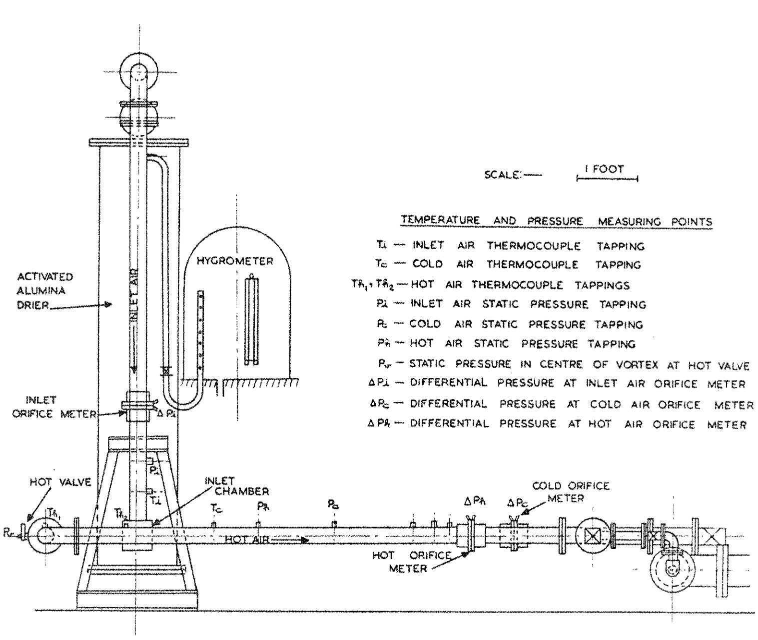

VORTEX TUBE APPARATUS GENERAL ASSEMBLY
FRONT VIEW.

FIG. 9.

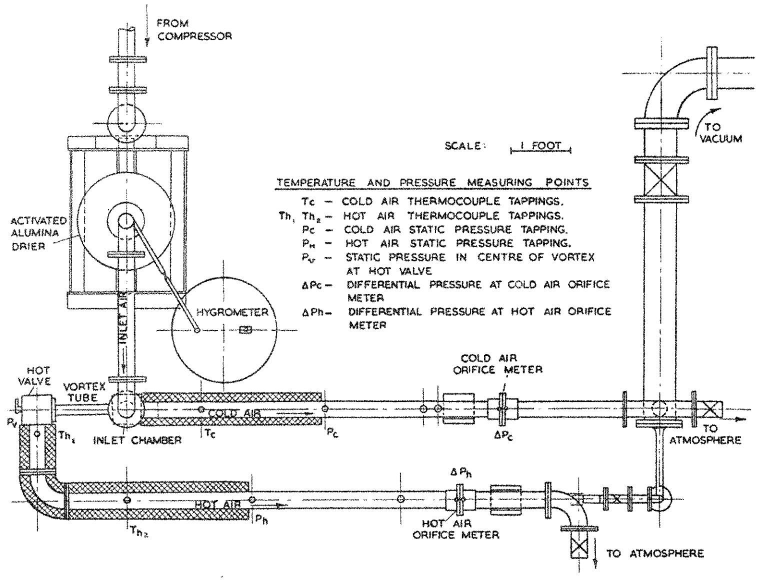

VORTEX TUBE APPARATUS GENERAL ASSEMBLY
PLAN VIEW.

FIG. 10.

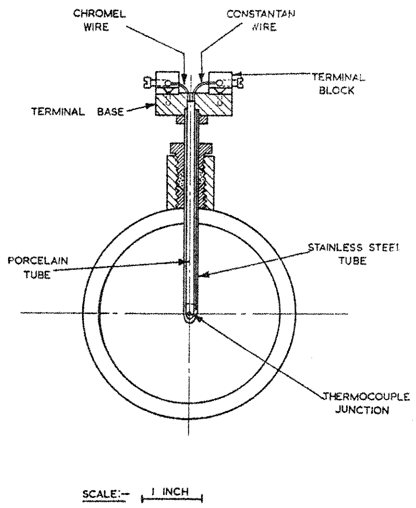

THERMOCOUPLE PROBE.

FIG. 11.

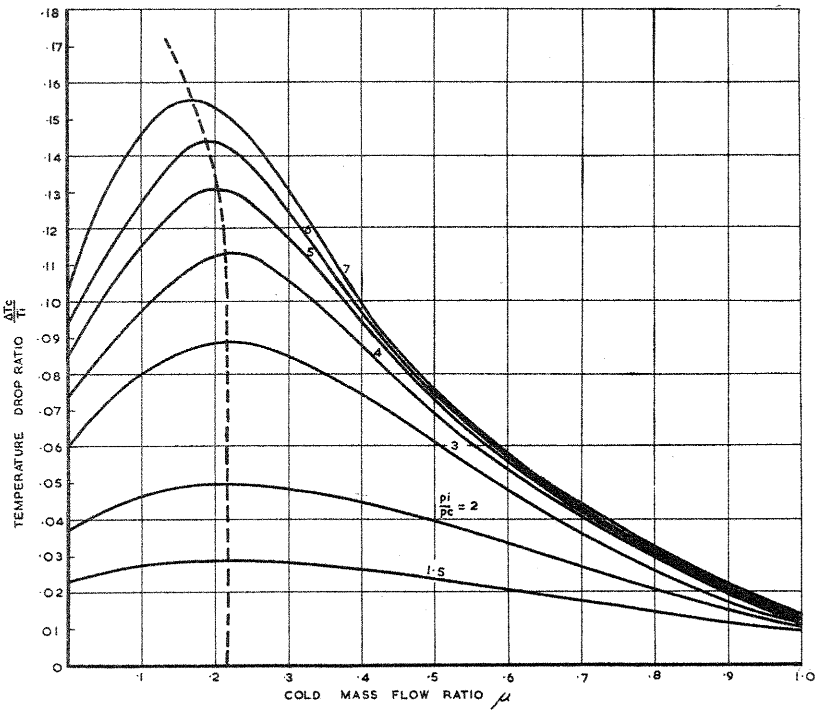

FIG 12 VARIATION OF TEMPERATURE DROP RATIO WITH COLD MASS FLOW RATIO FOR VARIOUS PRESSURE RATIOS.
$\frac{d_c}{D} = .250, \quad \frac{d_1}{D} = .266$

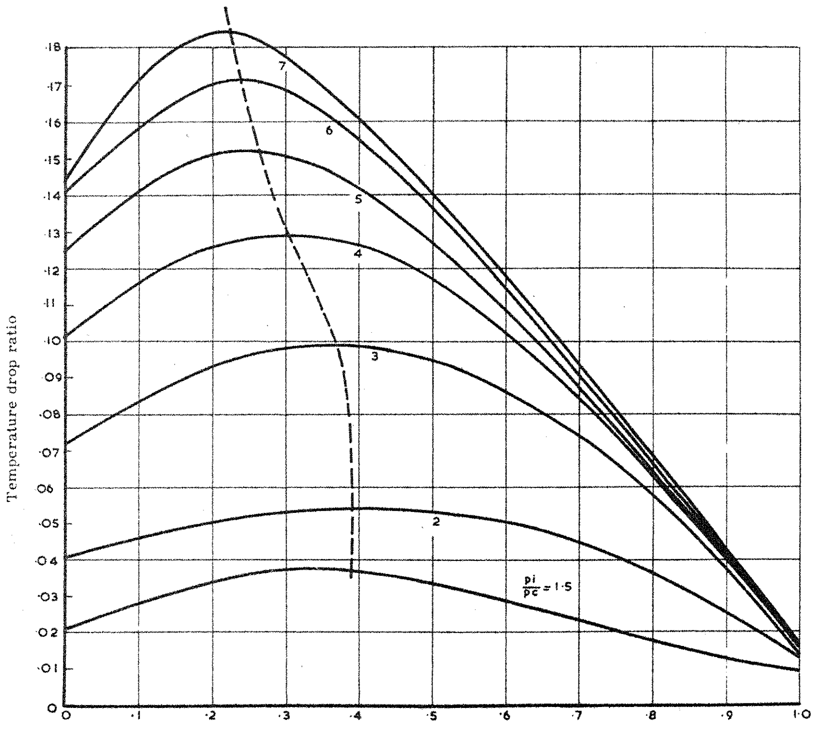

FIG. 13. VARIATION OF TEMPERATURE DROP RATIO WITH COLD MASS FLOW RATIO FOR VARIOUS PRESSURE RATIOS
$\frac{d_c}{D} = .333, \quad \frac{d_1}{D} = .266$

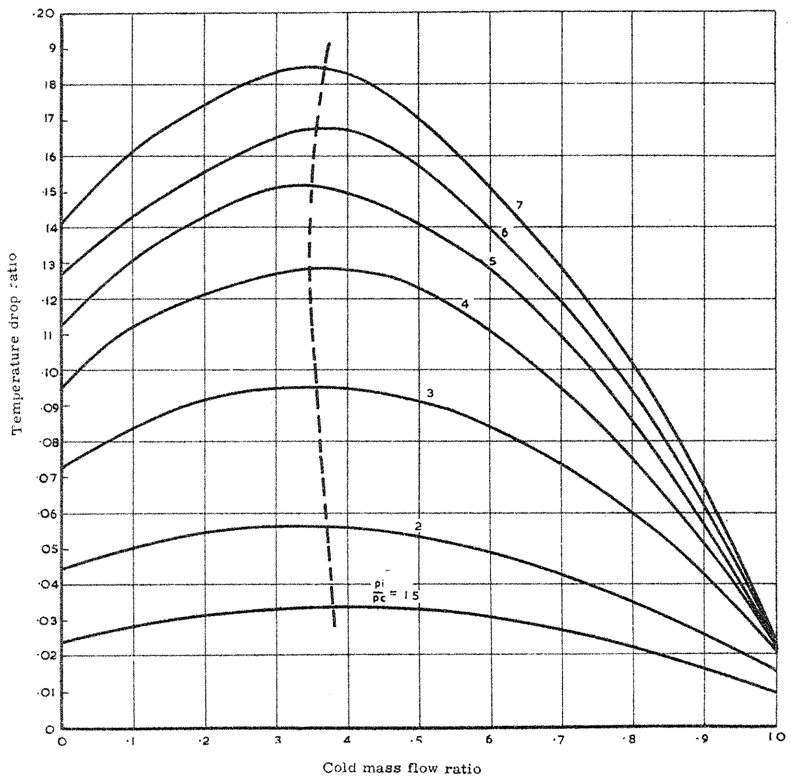

FIG. 14 VARIAT O\ OF TEMFERATURE DROP RATIO WITH COLD MASS FLO:V RAT :OR VARIOUS FRESSURE RATIOS

$\frac{d_c}{D}$ = 41 $\frac{d_1}{D}$ - 2 6

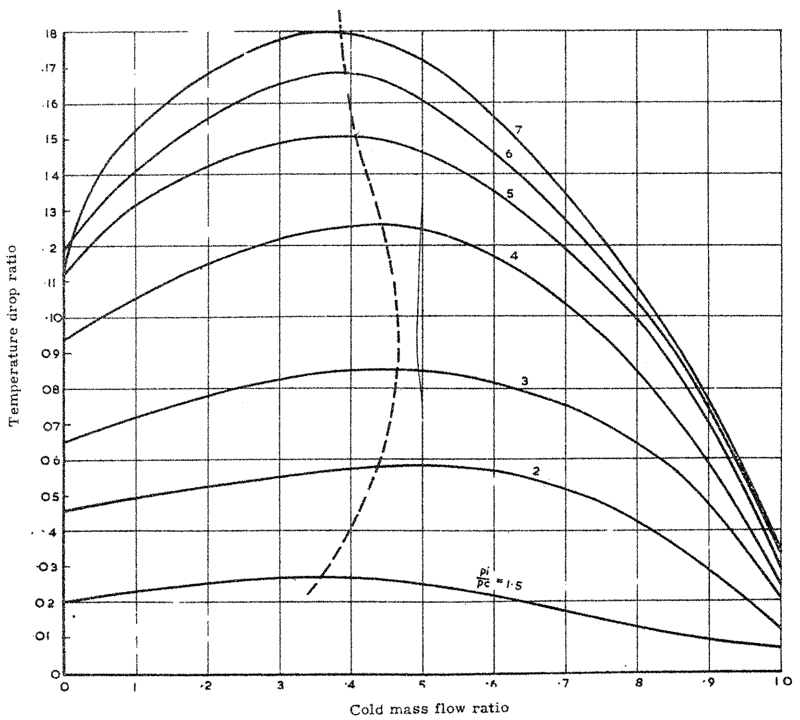

FIG 15 VARIATION OF TEMFERATURE DROP RATIO WITH COLD MASS FLOW RATIO FOR VARIOUS PRESSURE RATIOS

$\frac{d_c}{D}$ = .500, $\frac{d_1}{D}$ = 266

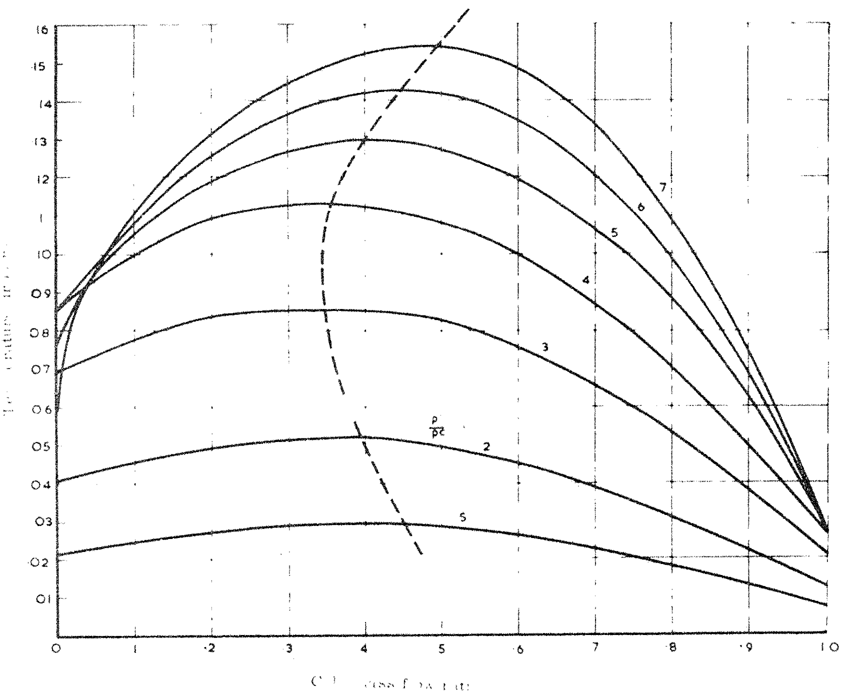

[illegible]

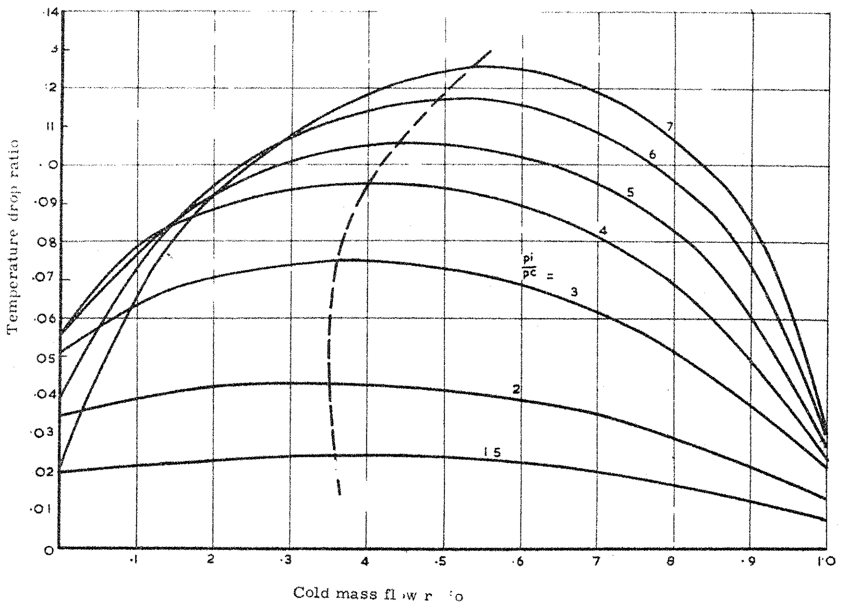

FIG. 17 VARIATION OF TEMPERATURE DROP RATIO WITH COLD MASS FLOW RATIO FOR VARIOUS PRESSURE RATIOS

$\frac{d_c}{D}$ = . 67, $\frac{d_i}{D}$ = . 266

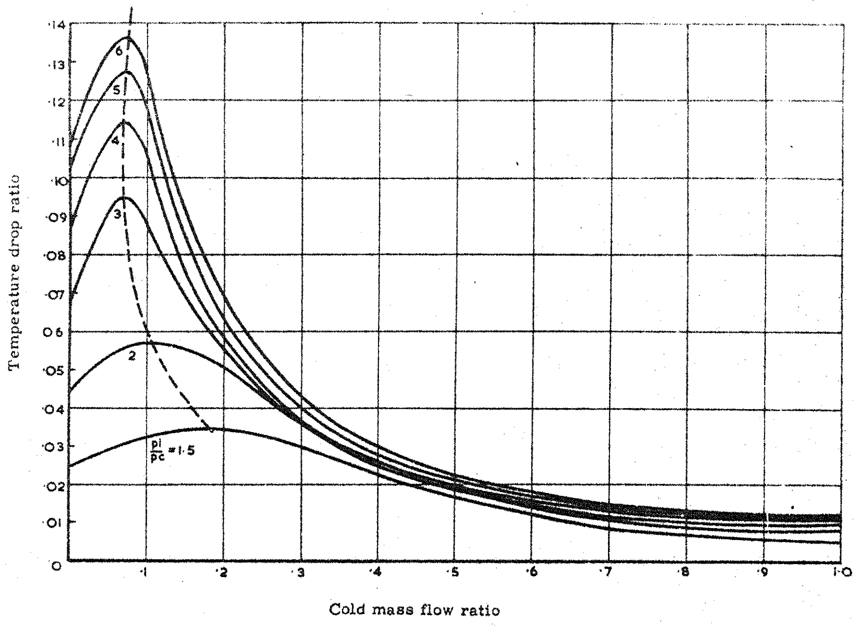

FIG. 18. VARIATION OF TEMPERATURE DROP RATIO WITH COLD MASS FLOW RATIO FOR VARIOUS PRESSURE RATIOS.
$\frac{d_c}{D}$ = .167, $\frac{d_i}{D}$ = .376

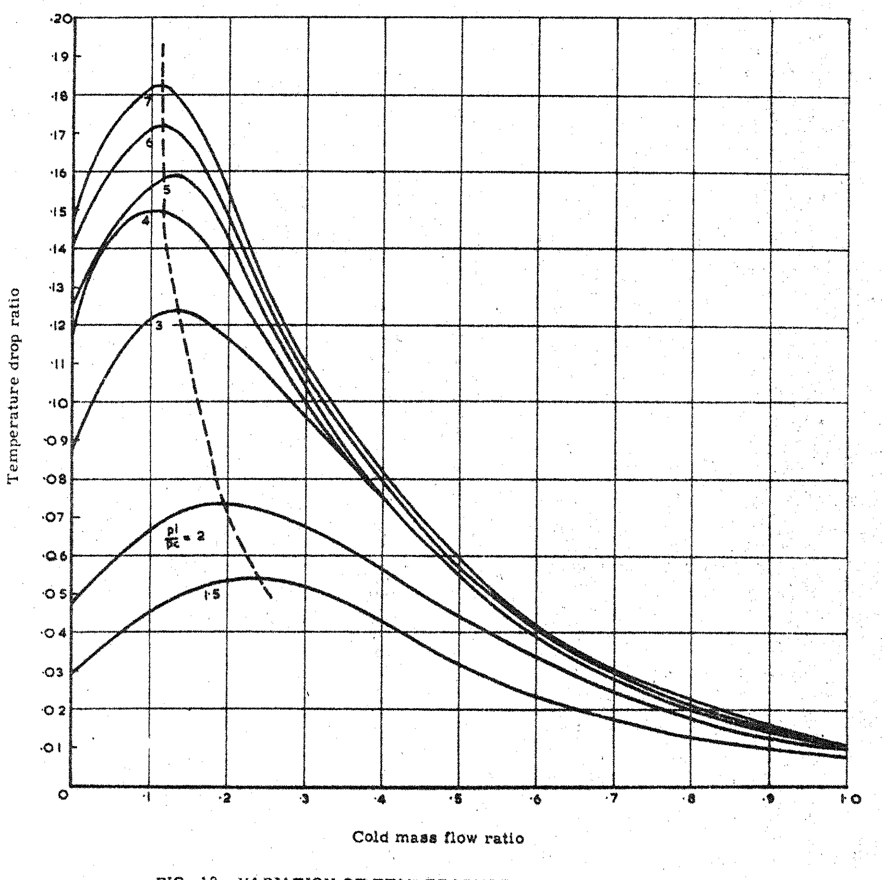

FIG. 19. VARIATION OF TEMPERATURE DROP RATIO WITH COLD MASS FLOW RATIO FOR VARIOUS PRESSURE RATIOS
$\frac{d_c}{D}$ = .250; $\frac{d_i}{D}$ = .376

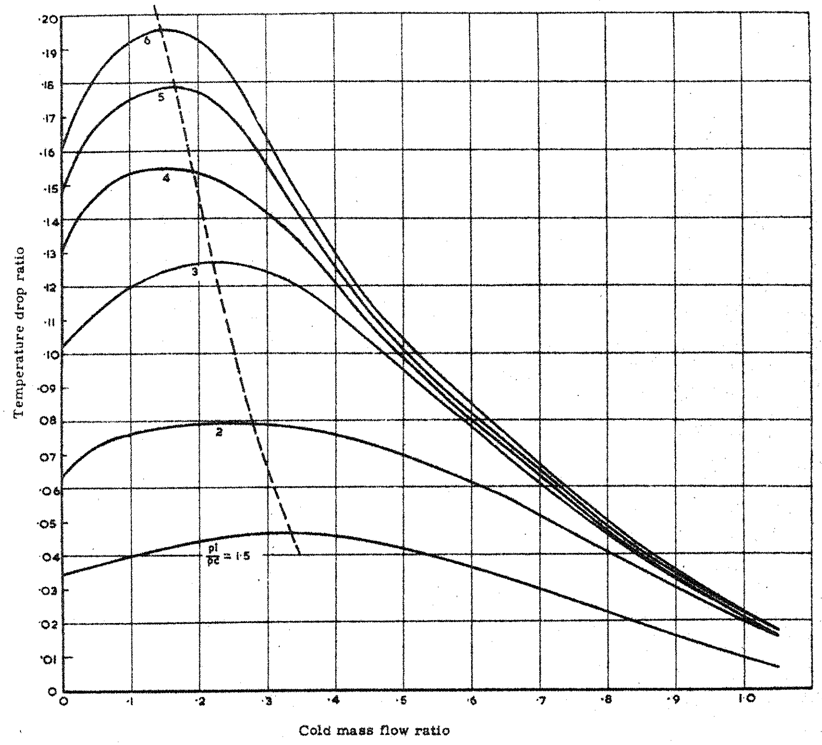

FIG. 20. VARIATION OF TEMPERATURE DROP RATIO WITH COLD MASS FLOW RATIO FOR VARIOUS PRESSURE RATIOS
$\frac{d_c}{D} = .333$; $\frac{d_i}{D} = .376$

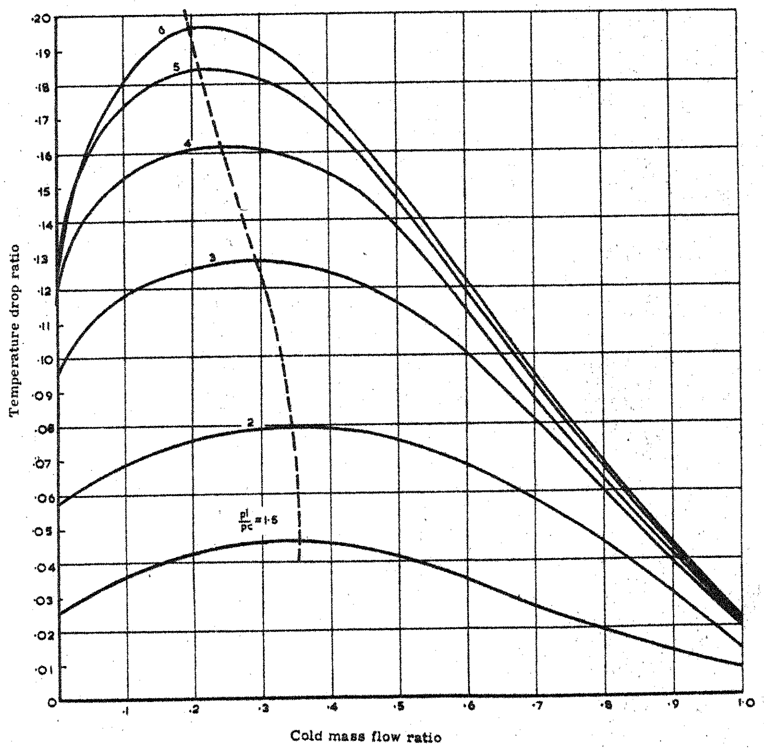

FIG. 21. VARIATION OF TEMPERATURE DROP RATIO WITH COLD MASS FLOW RATIO FOR VARIOUS PRESSURE RATIOS
$\frac{d_c}{D} = .417$; $\frac{d_i}{D} = .376$

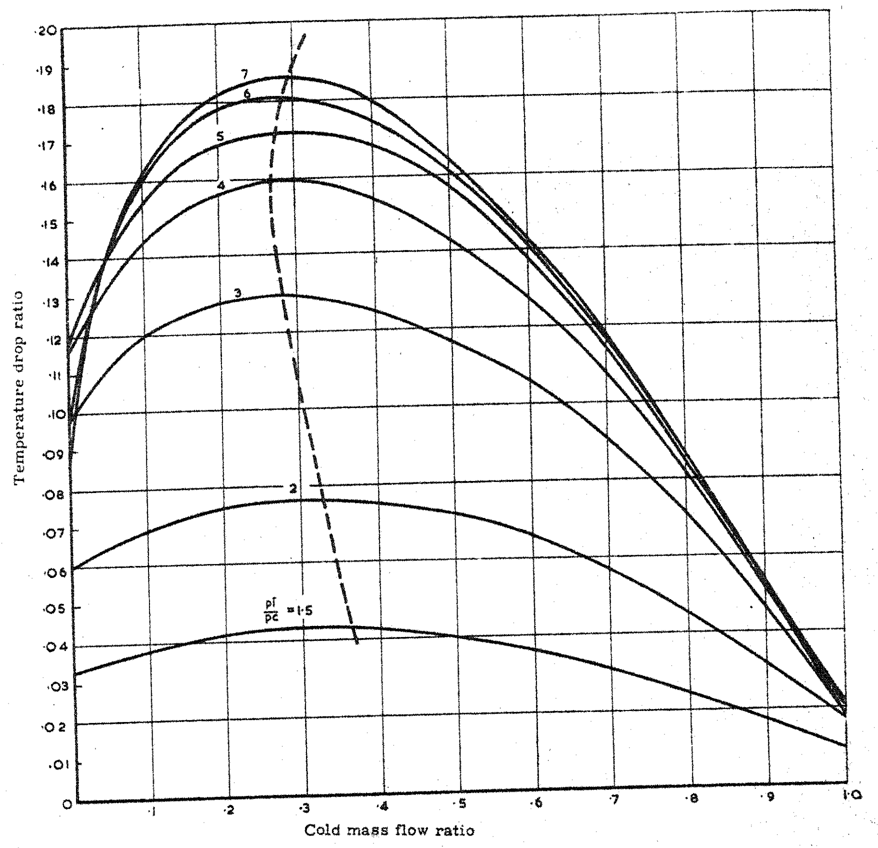

FIG. 22 VARIATION OF TEMPERATURE DROP RATIO WITH COLD MASS FLOW RATIO FOR VARIOUS PRESSURE RATIOS.
$\frac{d_c}{D}$ = . 550; $\frac{d_i}{D}$ = . 376

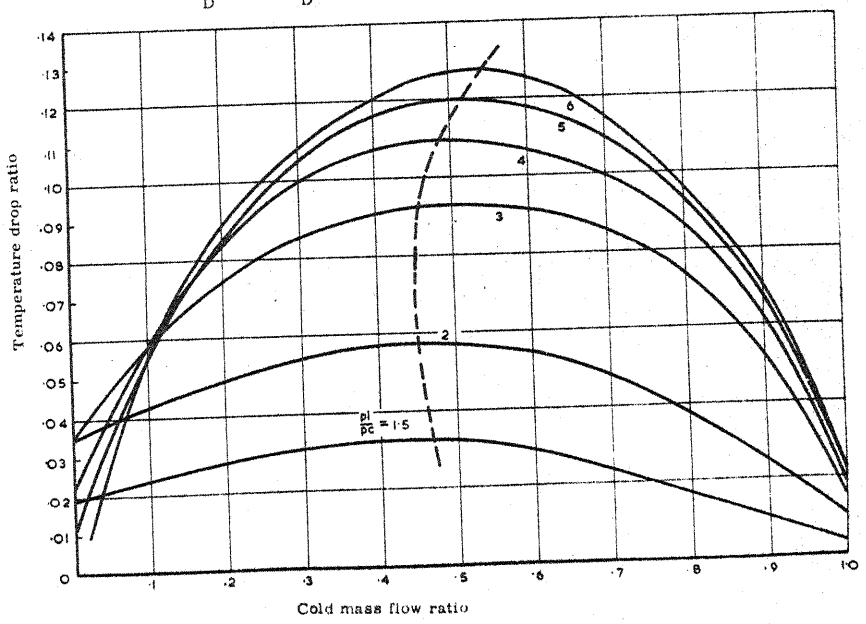

FIG. 23 VARIATION OF TEMPERATURE DROP RATIO WITH COLD MASS FLOW RATIO FOR VARIOUS PRESSURE RATIOS
$\frac{d_c}{D}$ = . 667, $\frac{d_i}{D}$ = . 376

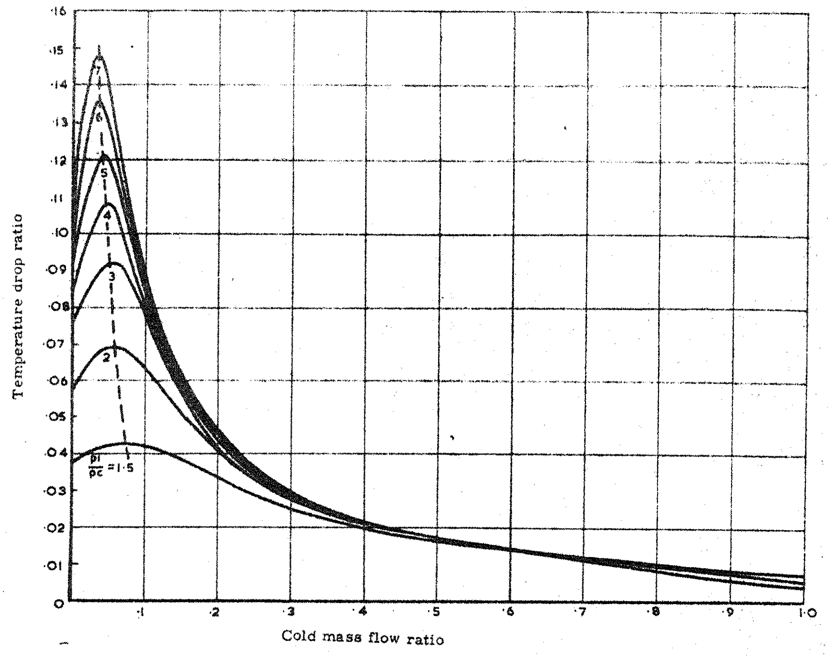

FIG. 24. VARIATION OF TEMPERATURE DROP RATIO WITH COLD MASS FLOW RATIO FOR VARIOUS PRESSURE RATIOS $\frac{d_c}{D} = .167$, $\frac{d_i}{D} = .461$

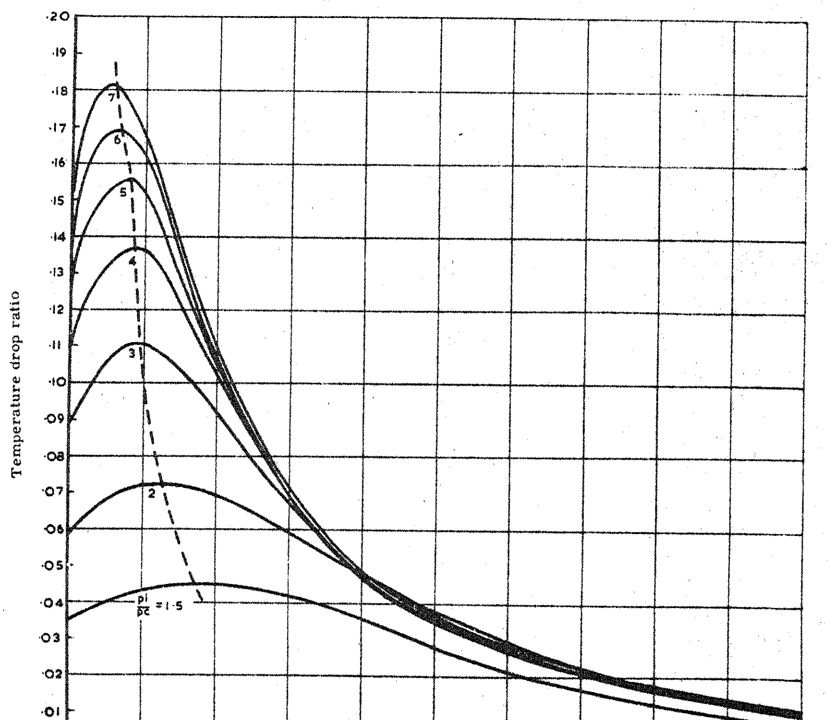

FIG. 25. VARIATION OF TEMPERATURE DROP RATIO WITH COLD MASS FLOW RATIO FOR VARIOUS PRESSURE RATIOS $\frac{d_c}{D} = .25$; $\frac{d_i}{D} = .461$

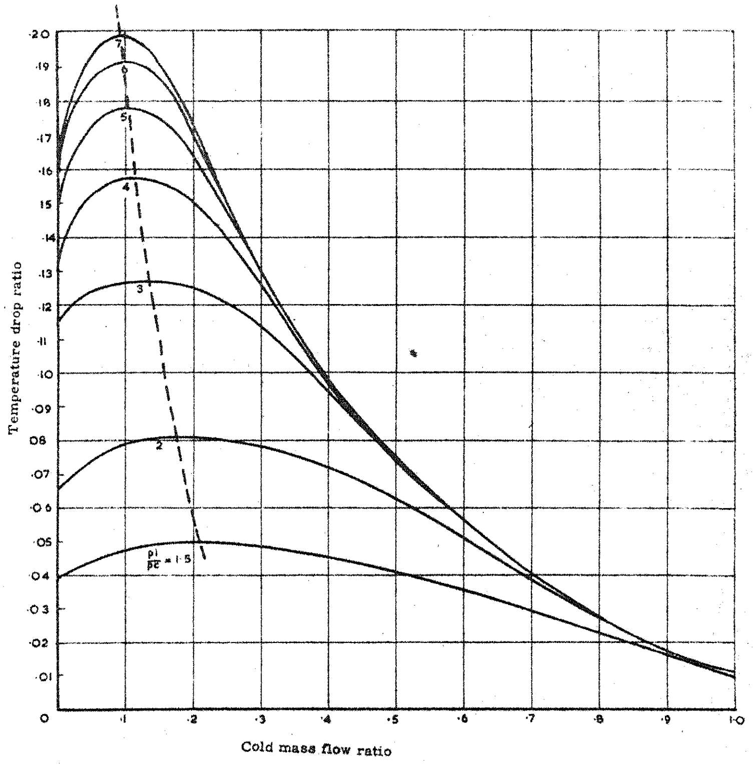

FIG. 26. VARIATION OF TEMPERATURE DROP RATIO WITH COLD MASS FLOW RATIO FOR VARIOUS PRESSURE RATIOS.
$\frac{d_c}{D}$ = .333; $\frac{d_i}{D}$ = .461

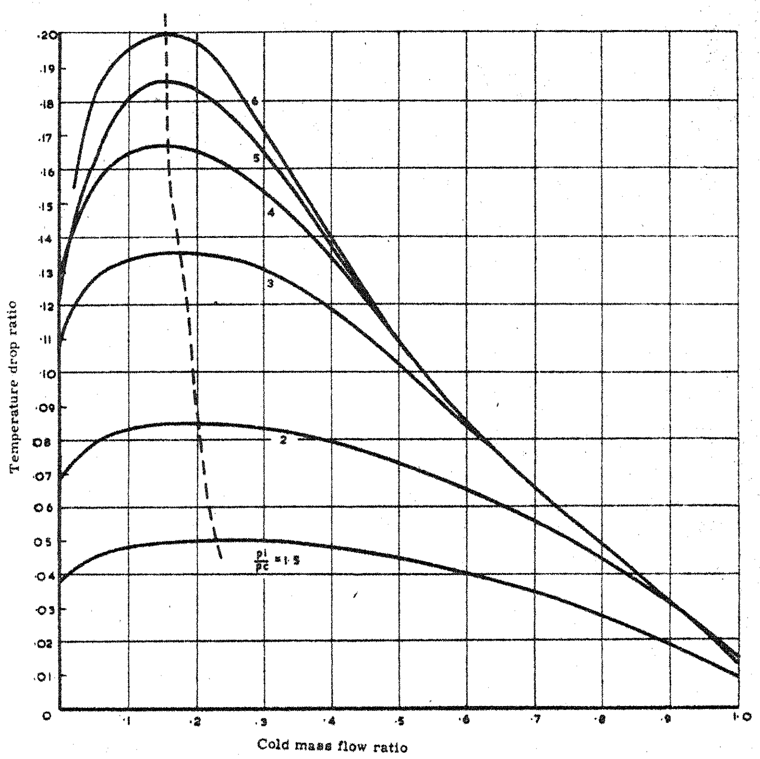

FIG. 27. VARIATION OF TEMPERATURE DROP RATIO WITH COLD MASS FLOW RATIO FOR VARIOUS PRESSURE RATIOS
$\frac{d_c}{D}$ = .417; $\frac{d_i}{D}$ = .461

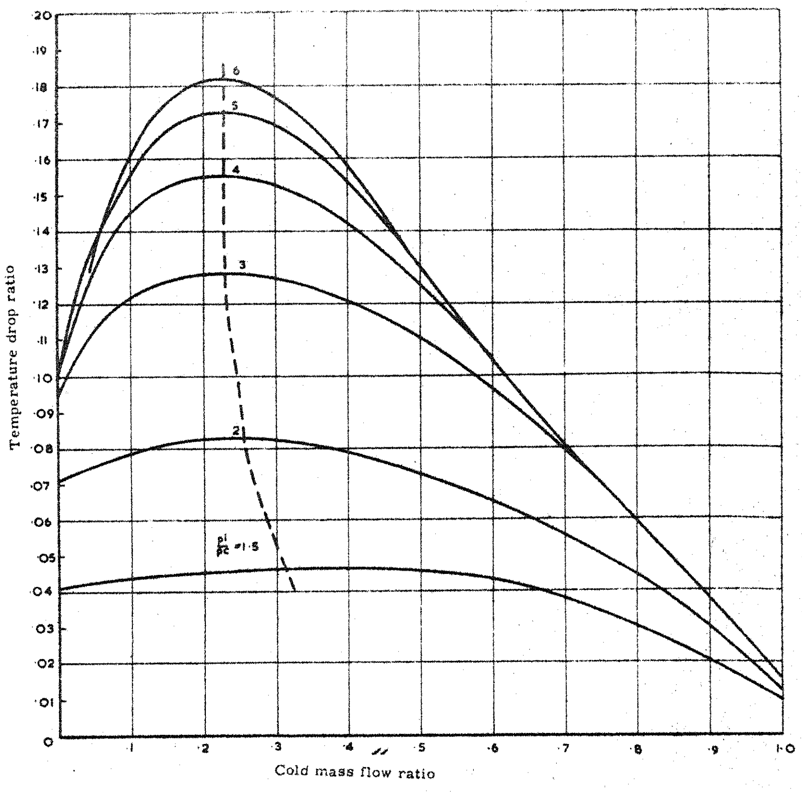

FIG. 28. VARIATION OF TEMPERATURE DROP RATIO WITH COLD MASS FLOW RATIO FOR VARIOUS PRESSURE RATIOS
$\frac{d_c}{D}$ = .500; $\frac{d_i}{D}$ = .461

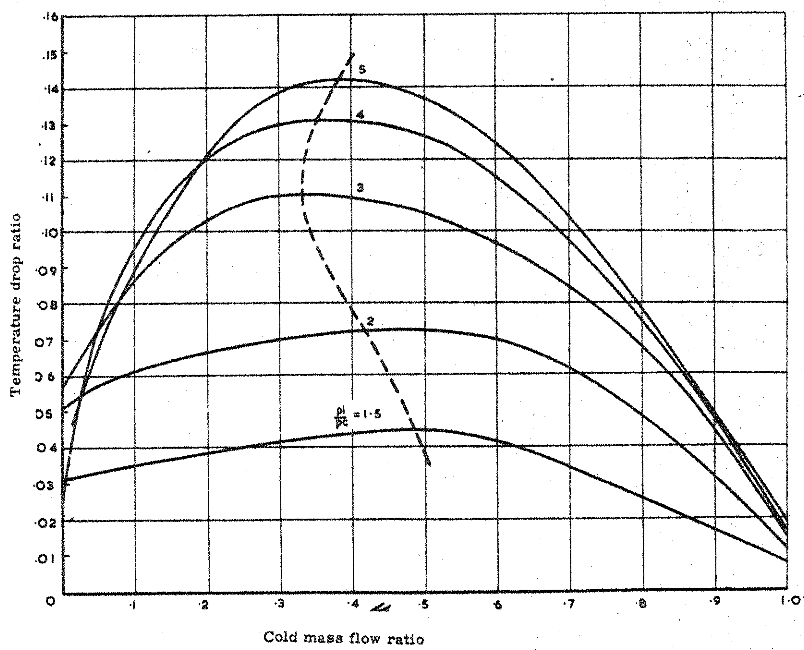

FIG. 29. VARIATION OF TEMPERATURE DROP RATIO WITH COLD MASS FLOW RATIO FOR VARIOUS PRESSURE RATIOS.
$\frac{d_c}{D}$ = .583, $\frac{d_i}{D}$ = .461

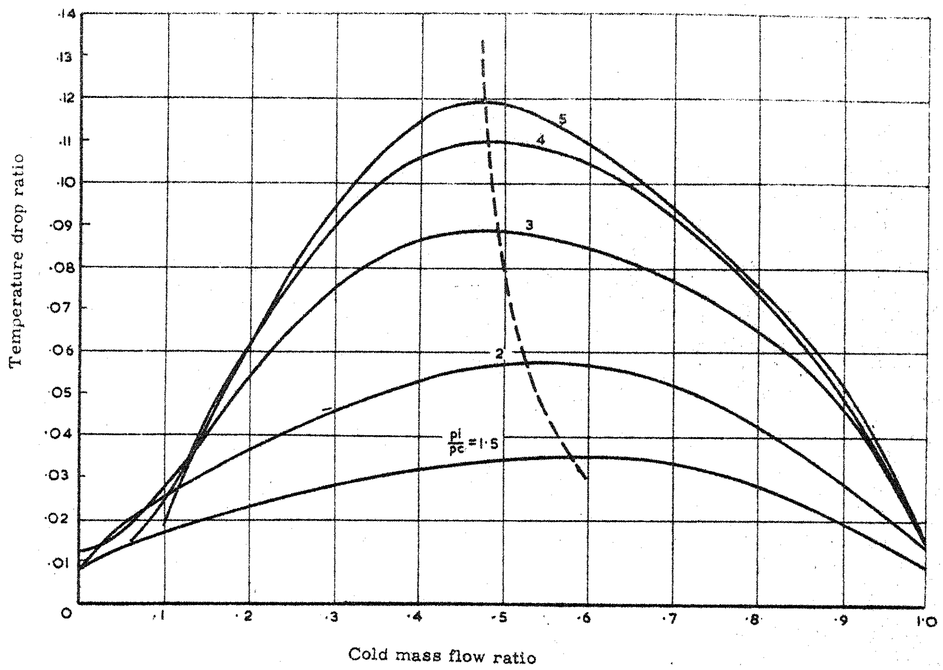

FIG. 30. VARIATION OF TEMPERATURE DROP RATIO WITH COLD MASS FLOW RATIO FOR VARIOUS PRESSURE RATIOS.
$\frac{d_c}{D} = .667, \quad \frac{d_i}{D} = .461$

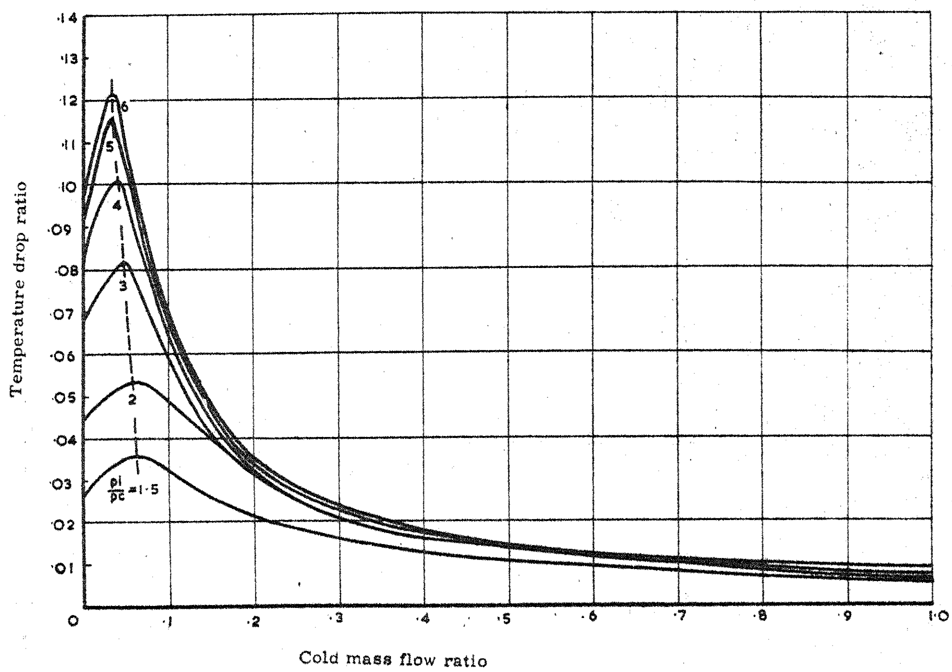

FIG. 31. VARIATION OF TEMPERATURE DROP RATIO WITH COLD MASS FLOW RATIO FOR VARIOUS PRESSURE RATIOS
$\frac{d_c}{D} = .167; \quad \frac{d_i}{D} = .532$

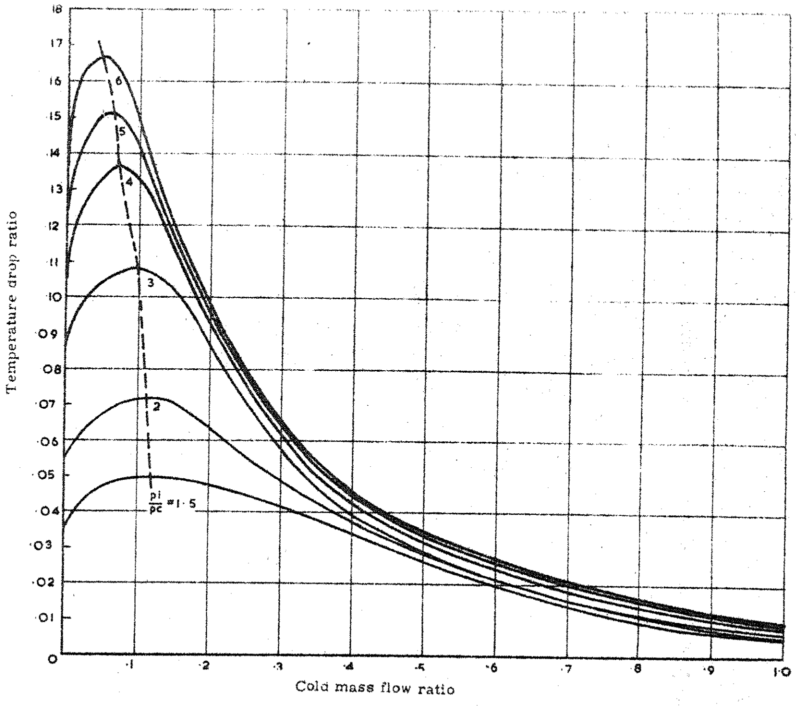

FIG. 32. VARIATION OF TEMPERATURE DROP RATIO WITH COLD MASS FLOW RATIO FOR VARIOUS PRESSURE RATIOS

$\frac{d_c}{D} = .250; \quad \frac{d_i}{D} = .532$

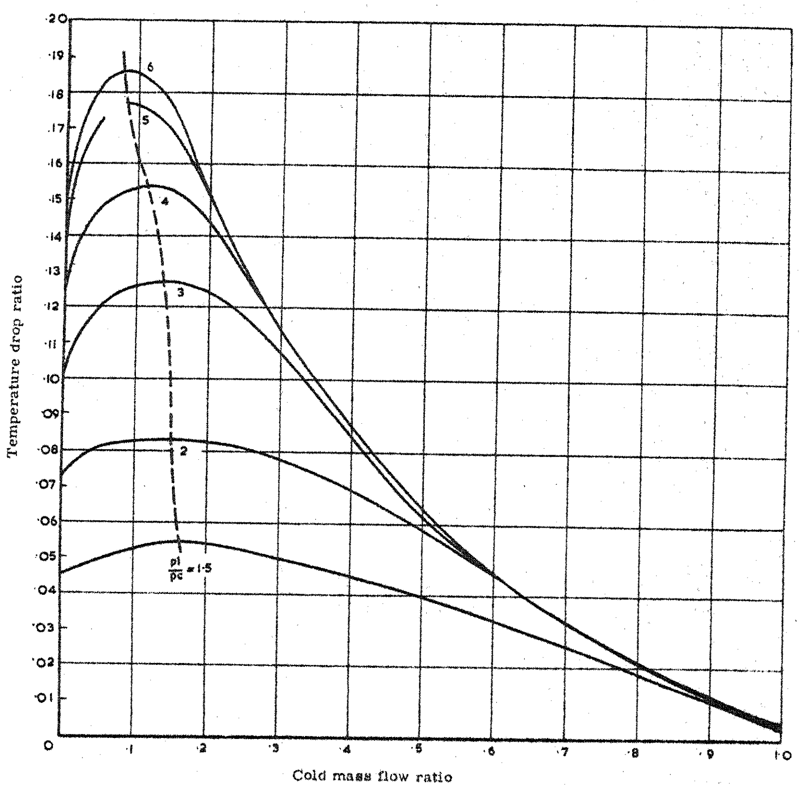

FIG. 33. VARIATION OF TEMPERATURE DROP RATIO WITH COLD MASS FLOW RATIO FOR VARIOUS PRESSURE RATIOS

$\frac{d_c}{D} = .333; \quad \frac{d_i}{D} = .532$

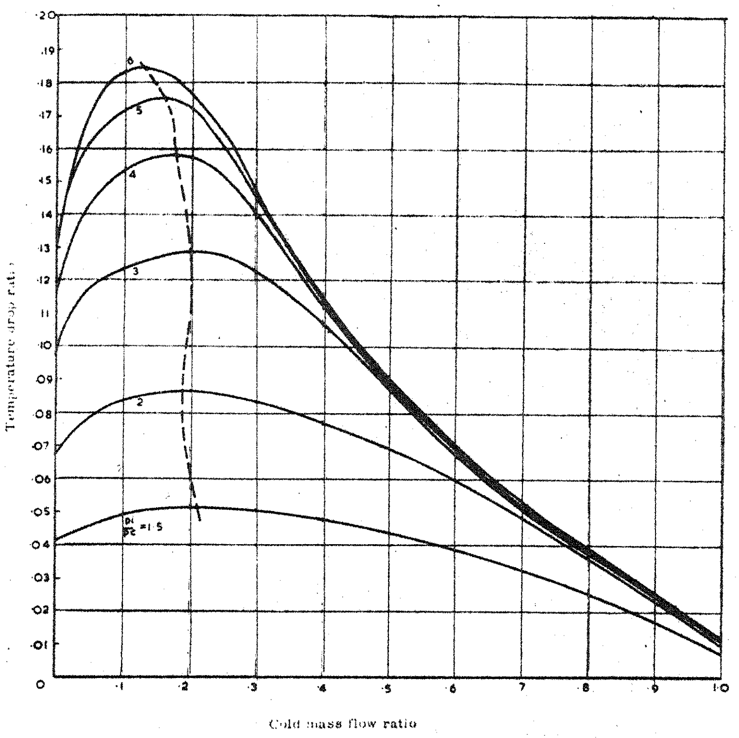

FIG. 34 VARIATION OF TEMPERATURE DROP RATIO WITH COLD MASS FLOW RATIO FOR VARIOUS PRESSURE RATIOS

$\frac{d_c}{D} = .417; \frac{d_i}{D} = .532$

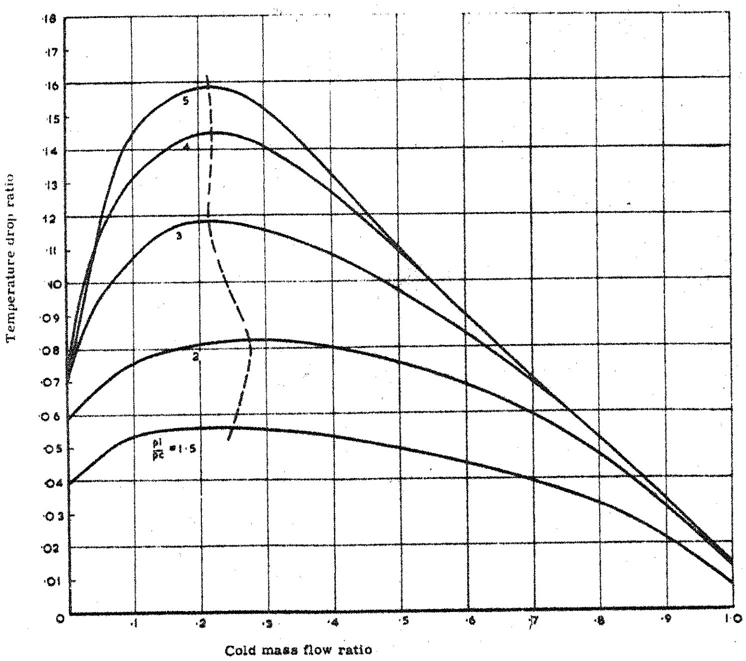

FIG. 35. VARIATION OF TEMPERATURE DROP RATIO WITH COLD MASS FLOW RATIO FOR VARIOUS PRESSURE RATIOS

$\frac{d_c}{D} = .500; \frac{d_i}{D} = .532$

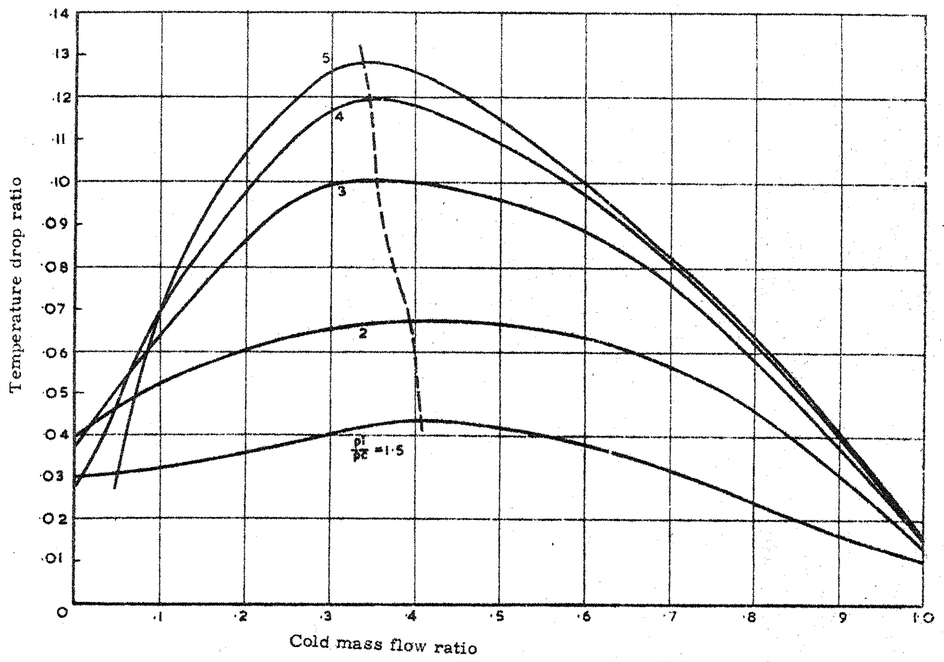

FIG. 36. VARIATION OF TEMPERATURE DROP RATIO WITH COLD MASS FLOW RATIO FOR VARIOUS PRESSURE RATIOS
$\frac{d_c}{D} = .583$; $\frac{d_i}{D} = .532$

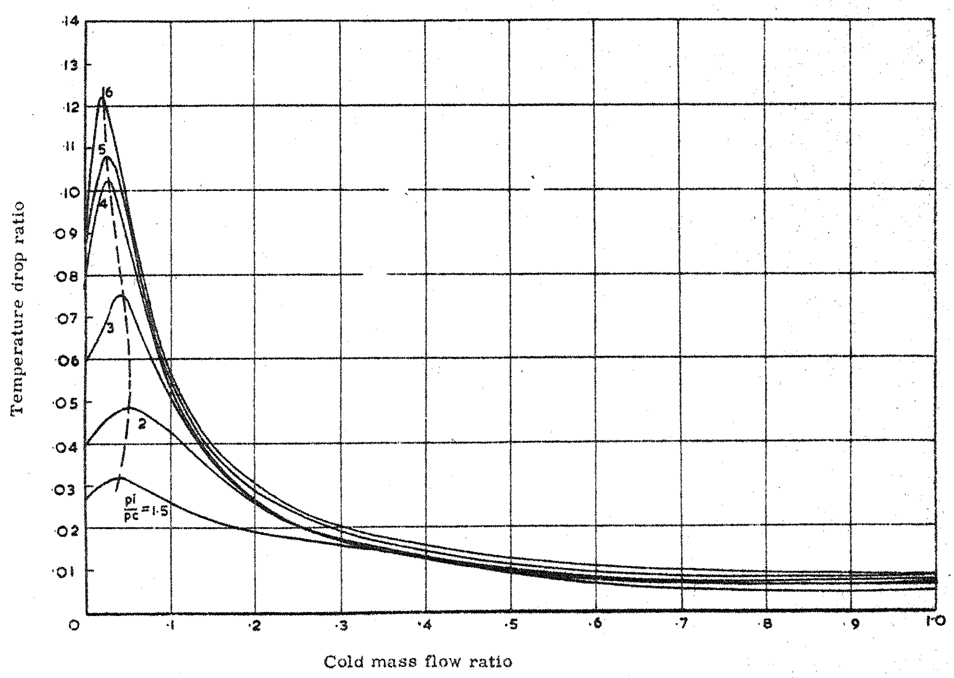

FIG. 37. VARIATION OF TEMPERATURE DROP RATIO WITH COLD MASS FLOW RATIO FOR VARIOUS PRESSURE RATIOS
$\frac{d_c}{D} = .167$; $\frac{d_i}{D} = .595$

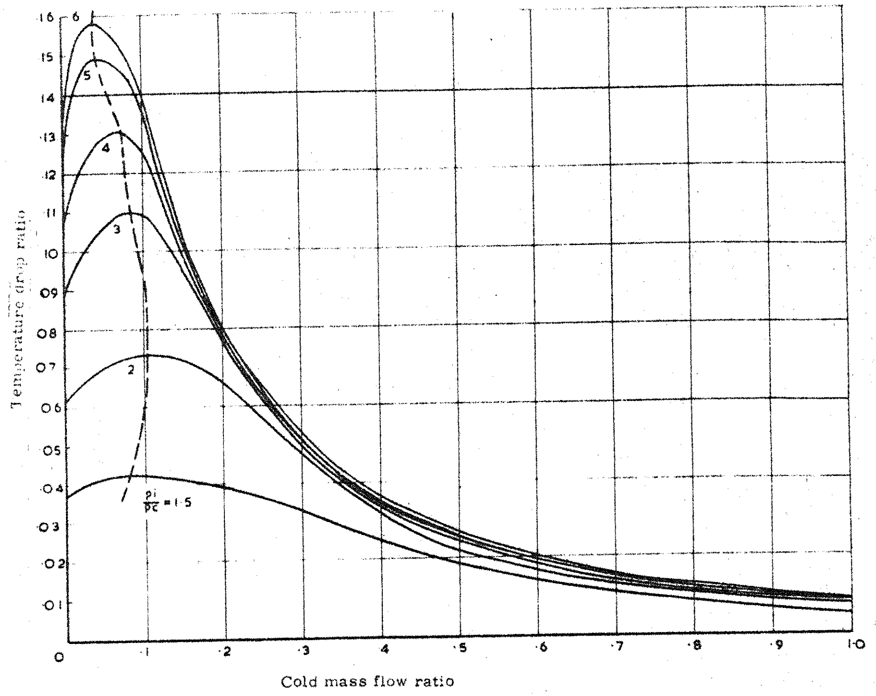

FIG. 38. VARIATION OF TEMPERATURE DROP RATIO WITH COLD MASS FLOW RATIO FOR VARIOUS PRESSURE RATIOS
$\frac{d_c}{D}$ = .250; $\frac{d_i}{D}$ = .595

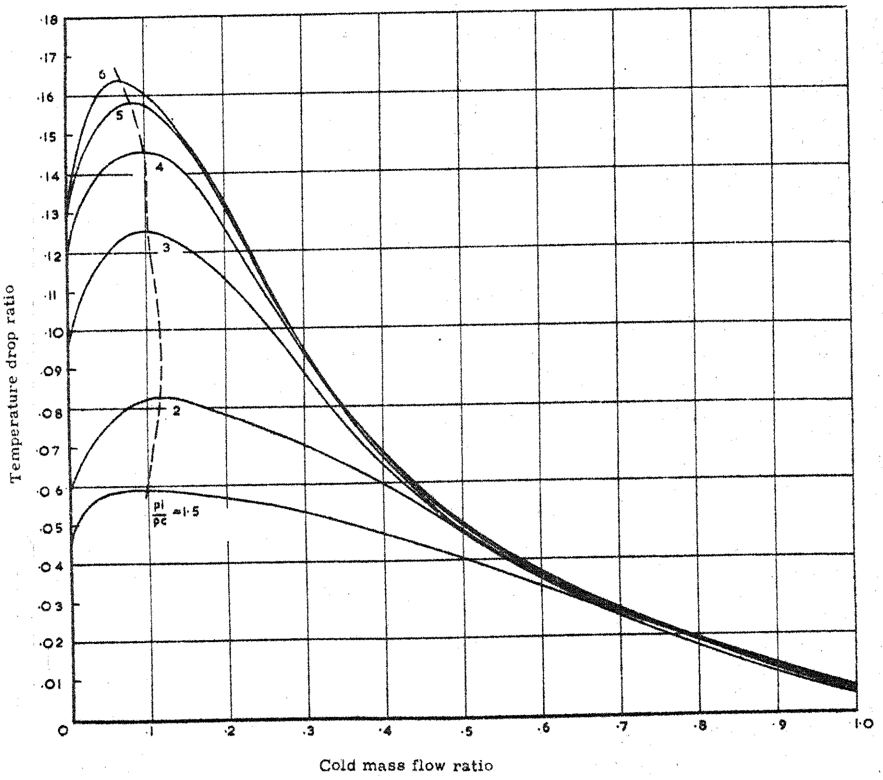

FIG. 39. VARIATION OF TEMPERATURE DROP RATIO WITH COLD MASS FLOW RATIO FOR VARIOUS PRESSURE RATIOS
$\frac{d_c}{D}$ = .333; $\frac{d_i}{D}$ = .595

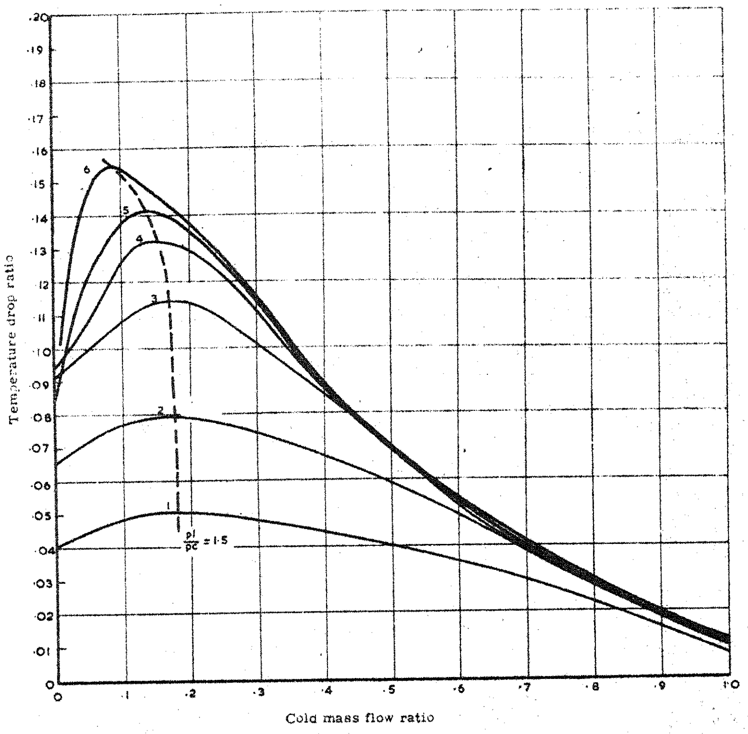

FIG. 40. VARIATION OF TEMPERATURE DROP RATIO WITH COLD MASS FLOW RATIO FOR VARIOUS PRESSURE RATIOS.

$\frac{d_c}{D} = .417, \quad \frac{d_i}{D} = .595$

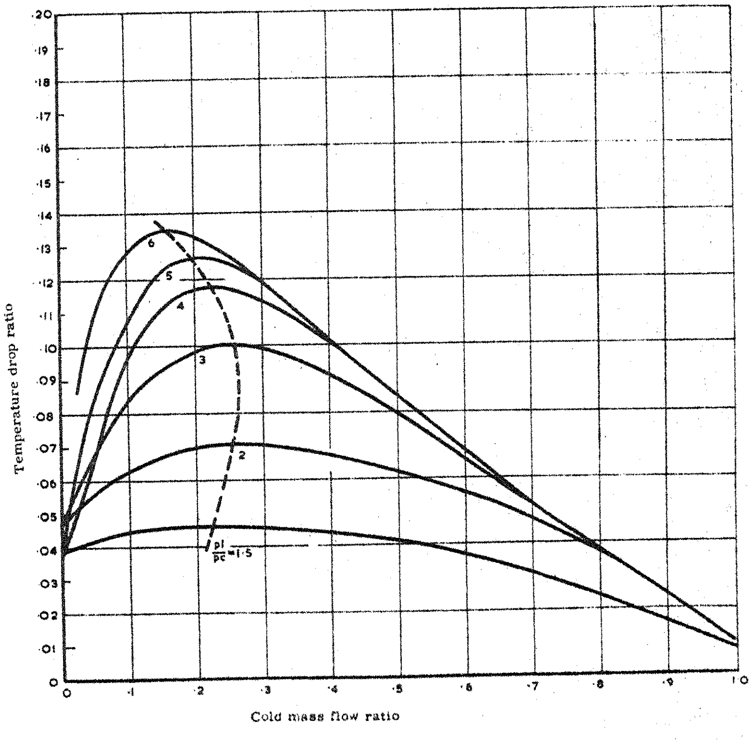

FIG. 41. VARIATION OF TEMPERATURE DROP RATIO WITH COLD MASS FLOW RATIO FOR VARIOUS PRESSURE RATIOS

$\frac{d_c}{D} = .500; \quad \frac{d_i}{D} = .595$

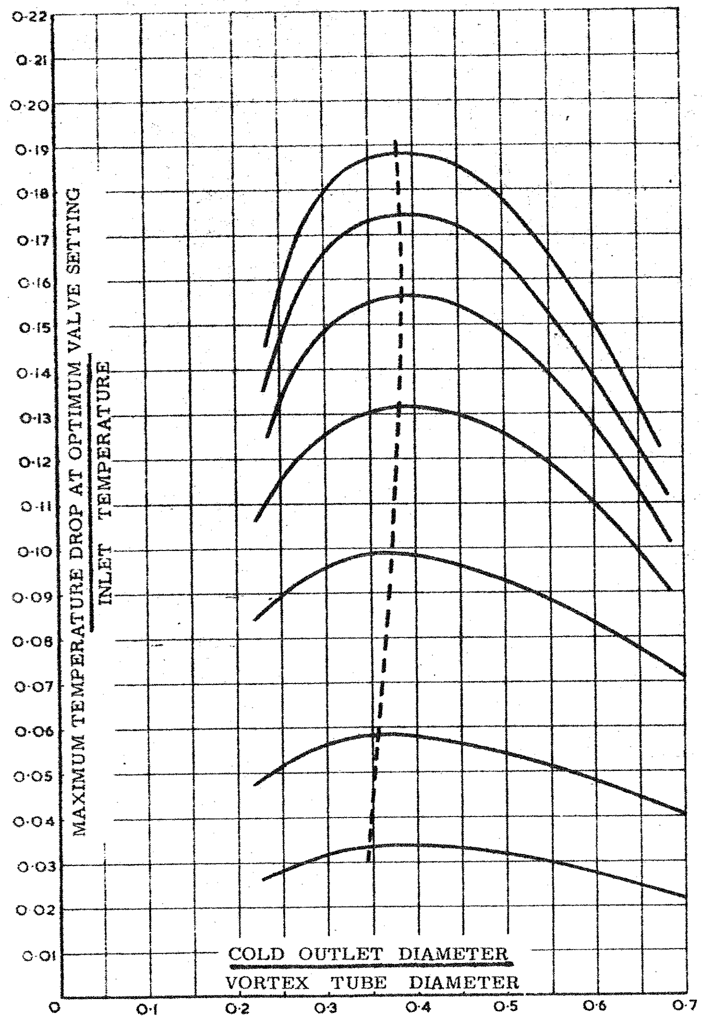

FIG. 42 VARIATION OF MAXIMUM TEMPERATURE DROP RATIO WITH COLD OUTLET DIAMETER RATIO FOR VARIOUS PRESSURE RATIOS.

$\frac{d_i}{D} = .266$

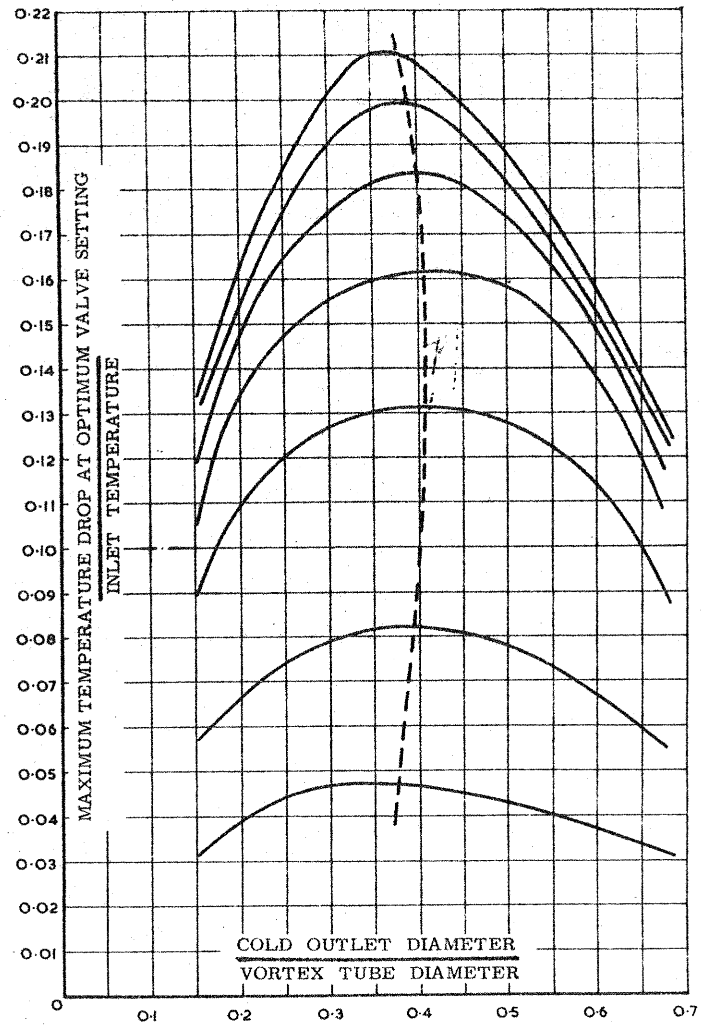

FIG. 43. VARIATION OF MAXIMUM TEMPERATURE DROP RATIO WITH COLD OUTLET DIAMETER RATIO FOR VARIOUS PRESSURE RATIOS.

$\frac{d_i}{D} = .376$

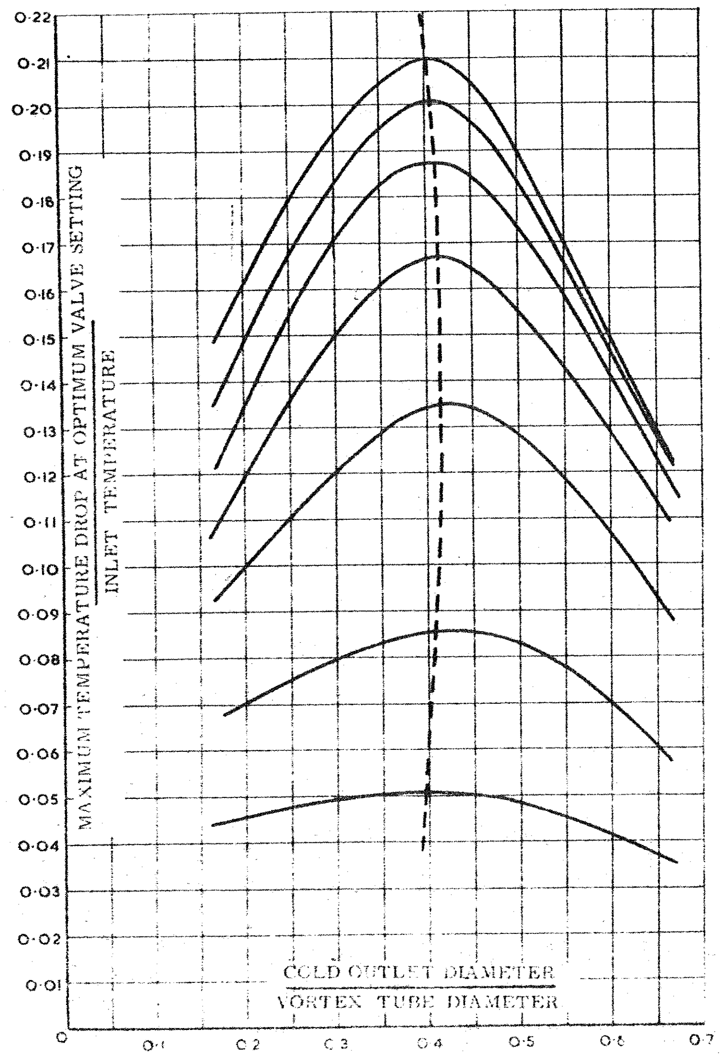

FIG. 44. VARIATION OF MAXIMUM TEMPERATURE DROP RATIO WITH COLD OUTLET DIAMETER RATIO FOR VARIOUS PRESSURE RATIOS.

$\frac{d}{D}$ = ·4 [illegible]

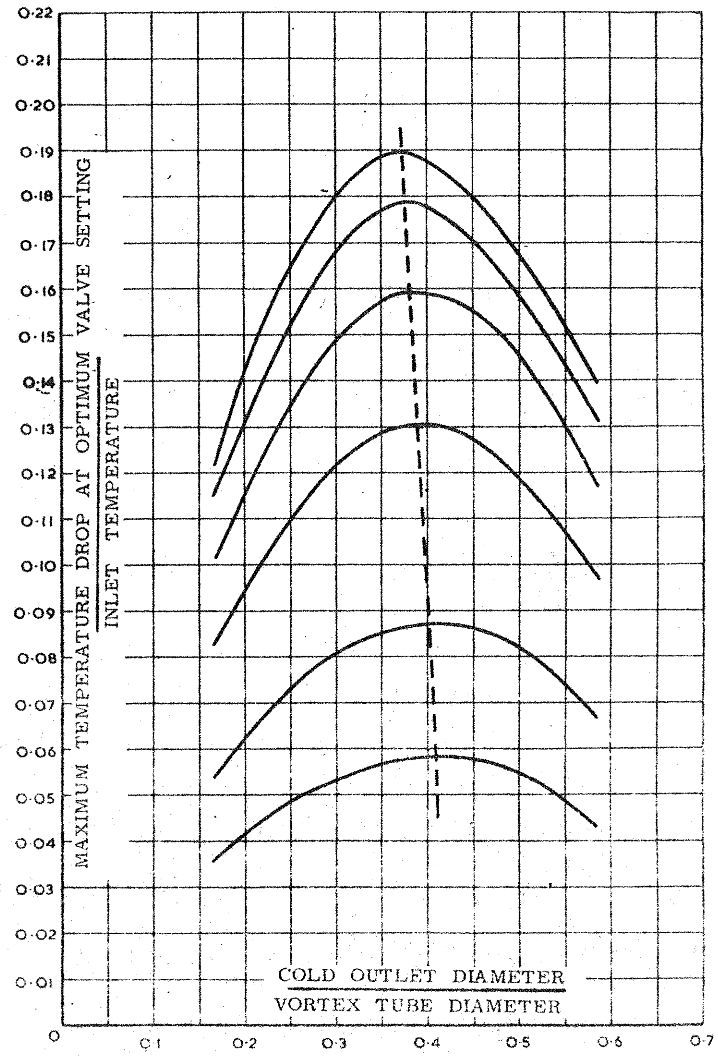

FIG. 45. VARIATION OF MAXIMUM TEMPERATURE DROP RATIO WITH COLD OUTLET DIAMETER RATIO FOR VARIOUS PRESSURE RATIOS.

$\frac{d}{D} = .332$

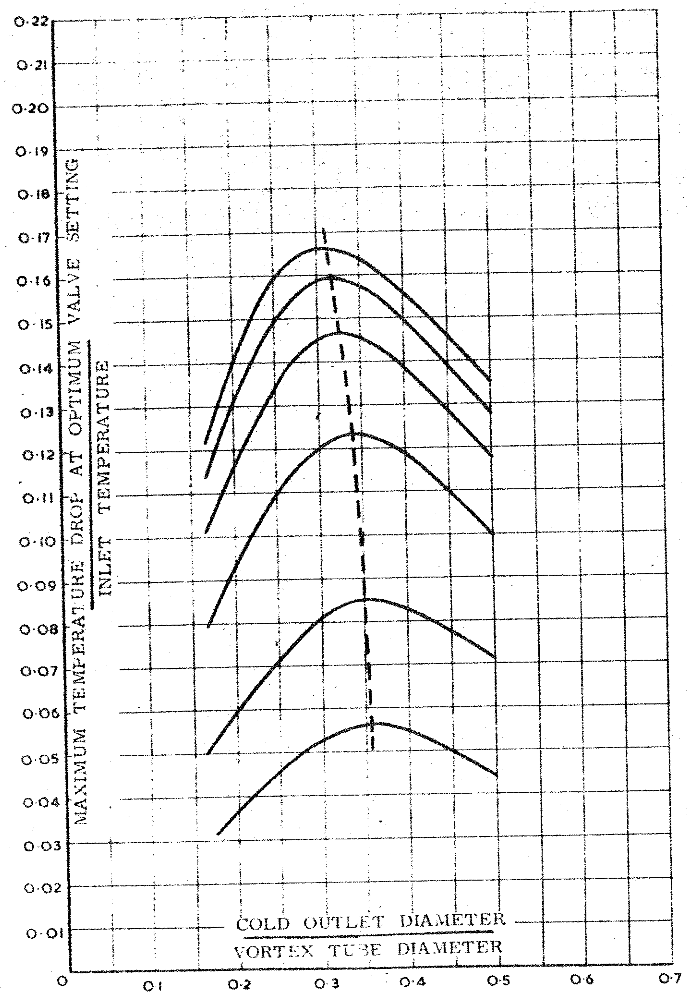

FIG. 46. VARIATION OF MAXIMUM TEMPERATURE DROP RATIO WITH COLD OUTLET DIAMETER RATIO FOR VARIOUS PRESSURE RATIOS

$\frac{d_i}{D}$ = .595

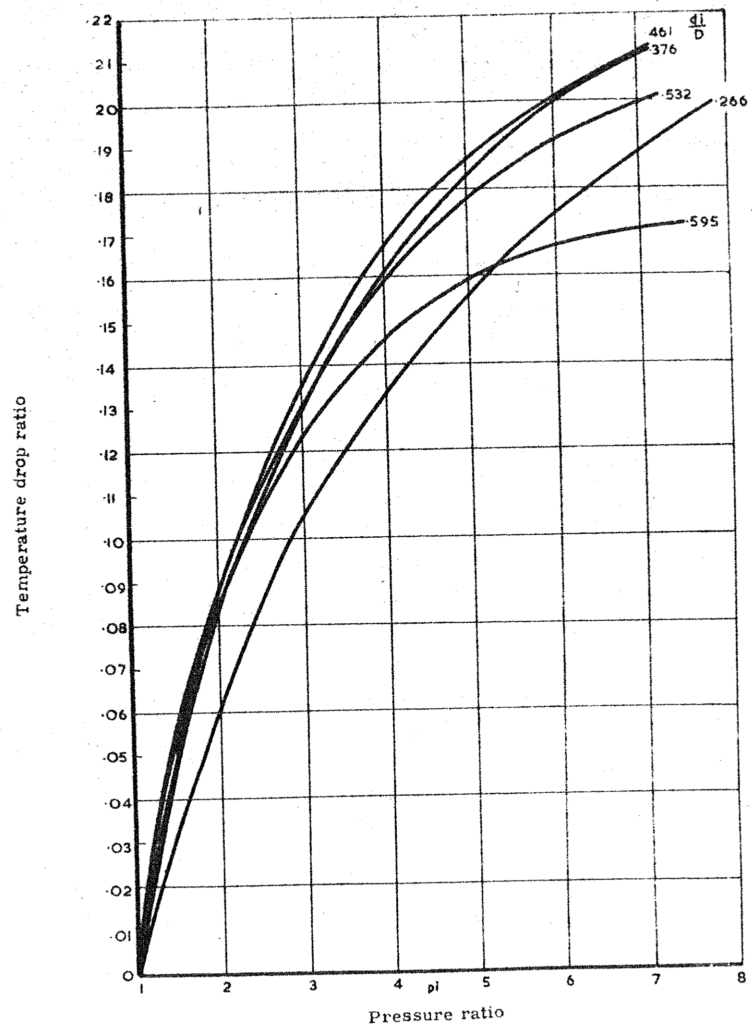

Fig. 47. VARIATION OF TEMPERATURE DROP RATIO WITH PRESSURE RATIO FOR OPTIMUM COLD OUTLET DIAMETER, OPTIMUM VALUE SETTING AND GIVEN INLET SIZE $\frac{d_i}{D}$

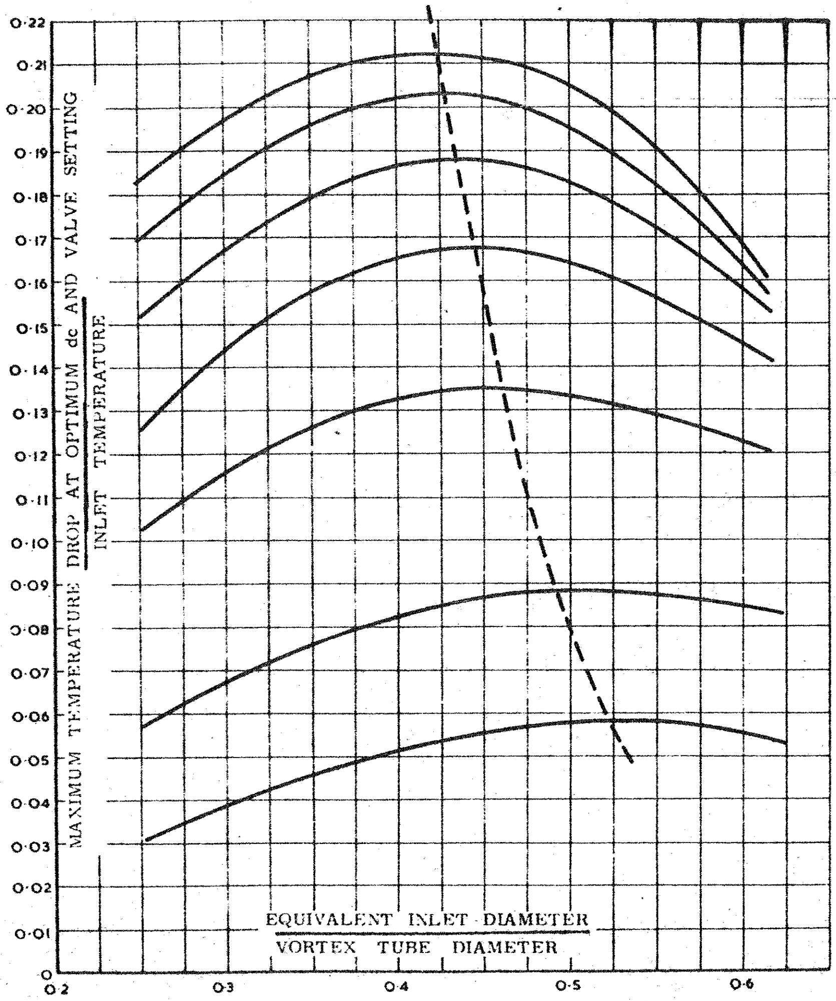

FIG. 48. VARIATION OF TEMPERATURE DROP RATIO WITH INLET SIZE FOR OPTIMUM COLD OUTLET AND VALVE SETTING

$\frac{p_i}{p_c}$ = 1.5, 2.0, 3.0, 4.0, 5.0, 6.0, 7.0

$$\left(\frac{\Delta T_c}{T_i}\right)_2 \sim \frac{di}{D}$$

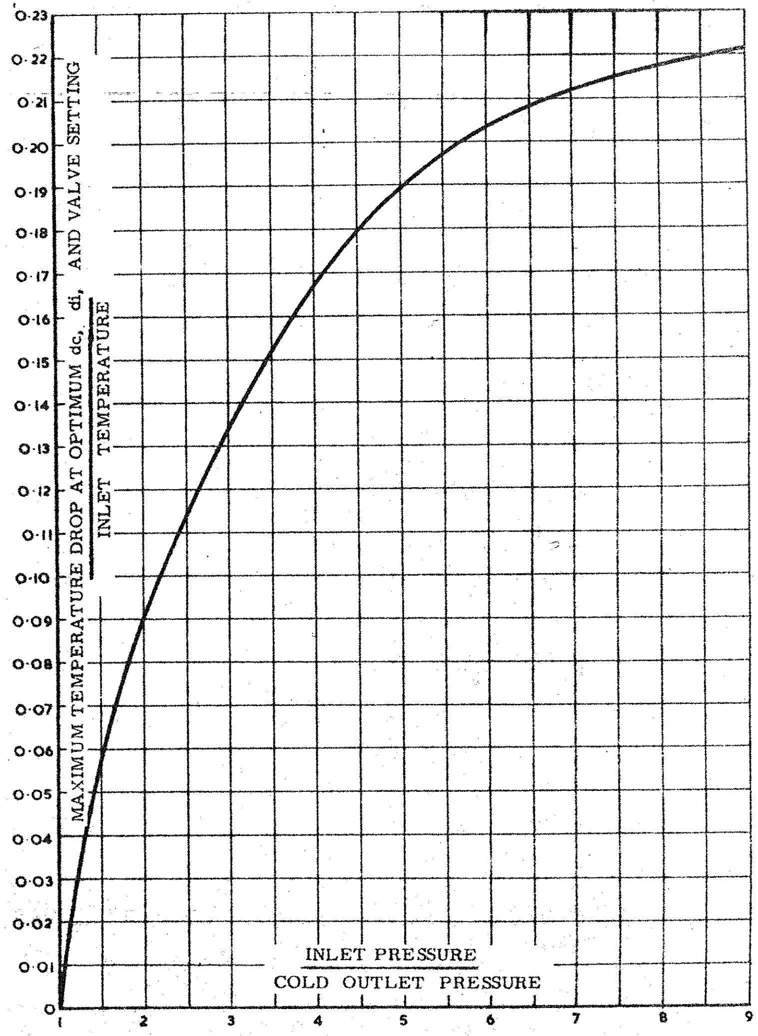

FIG. 49. VARIATION OF TEMPERATURE DROP EFFICIENCY WITH PRESSURE RATIO AT OPTIMUM COLD OUTLET SIZE, OPTIMUM VALVE SETTING AND FIXED INLET DIAMETER.

$\frac{d_i}{D}$ = .266, .376, .461, .532, .595

$$\frac{\Delta T_{c_2}}{\Delta T_{c\ ISEN}} \sim \frac{p_i}{p_c}$$

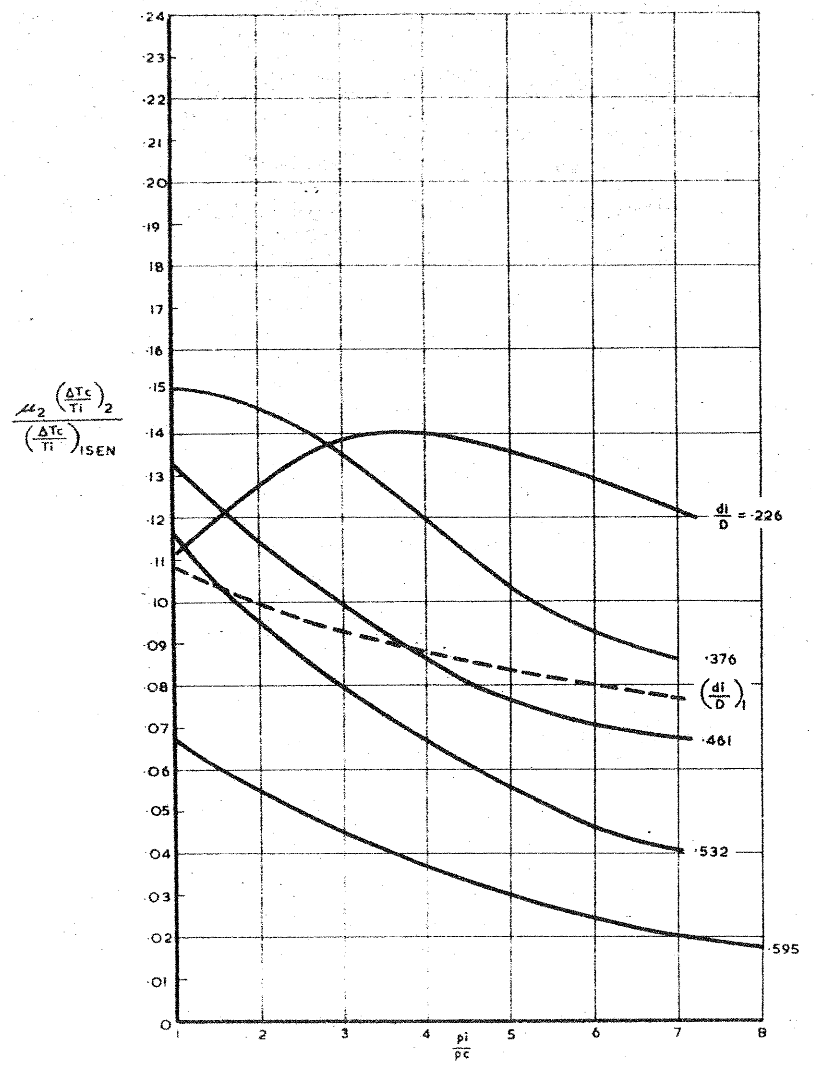

FIG. 5[illegible] VARIATION OF REFRIGERATION EFFICIENCY WITH PRESSURE RATIO AT OPTIMUM VALVE SETTING AND COLD OUTLET DIAMETER FOR MAXIMUM TEMPERATURE DROP RATIO.

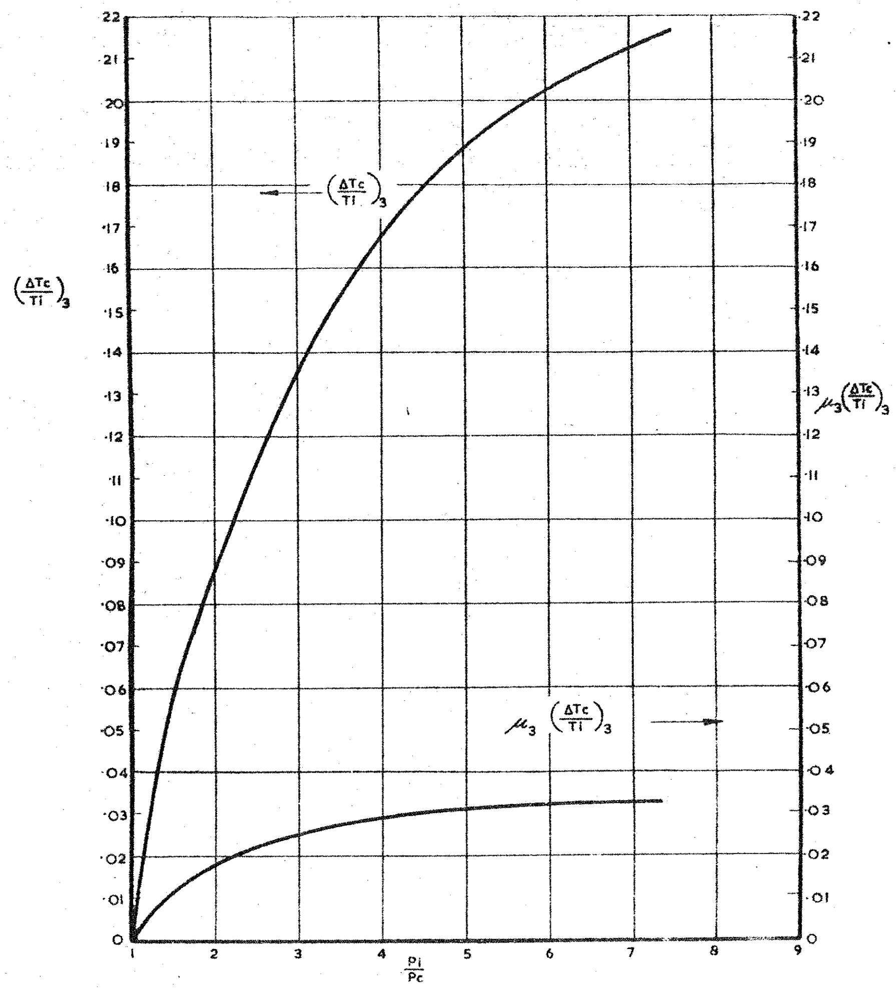

FIG. 51. VARIATION OF TEMPERATURE DROP RATIO AND REFRIGERATION RATIO WITH PRESSURE RATIO AT MAXIMUM TEMPERATURE DROP AND OPTIMUM CONDITIONS.

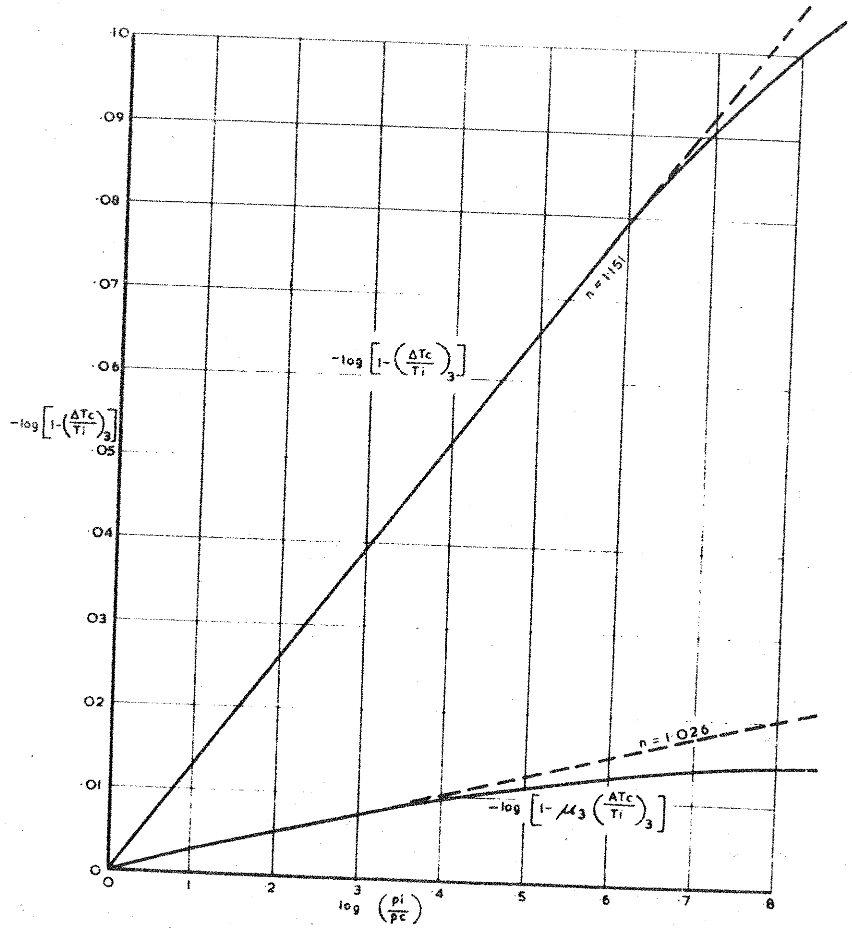

FIG. 52. POWER LAW VARIATION OF TEMPERATURE DROP RATIO AND REFRIGERATION RATE WITH PRESSURE RATIO AT MAXIMUM TEMPERATURE DROP.

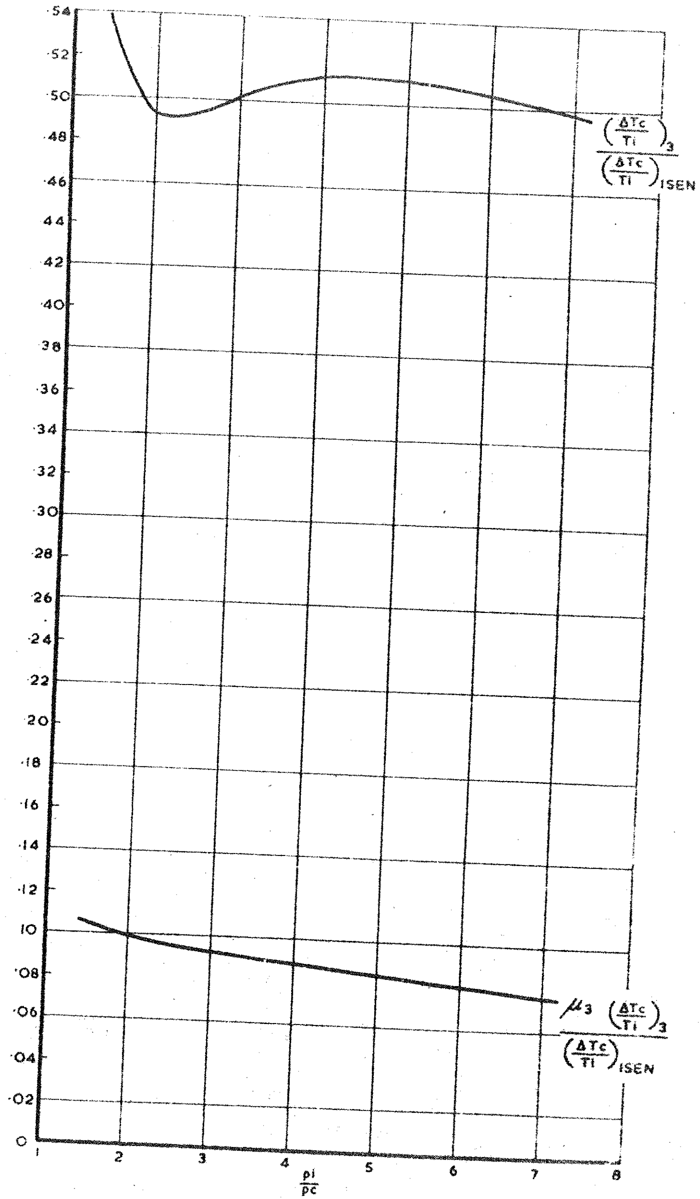

FIG. 52. VARIATION OF TEMPERATURE DROP EFFICIENCY AND REFRIGERATION EFFICIENCY WITH PRESSURE RATIO AT MAXIMUM TEMPERATURE DROP.

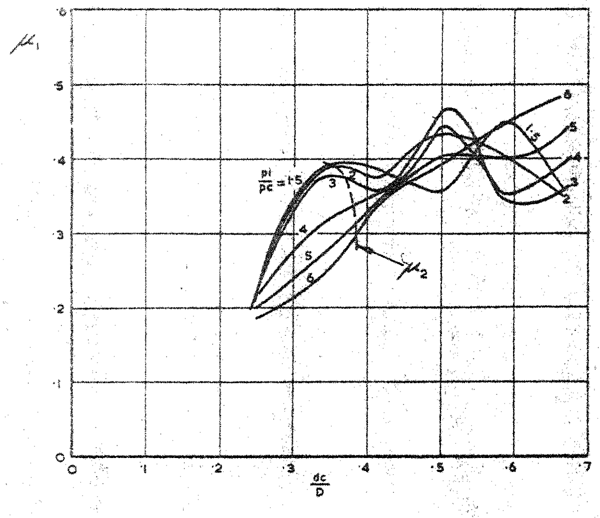

FIG. 54. VARIATION OF COLD MASS FLOW RATIO WITH COLD OUTLET DIAMETER RATIO AT OPTIMUM VALVE SETTING $\frac{d_i}{D} = .266$

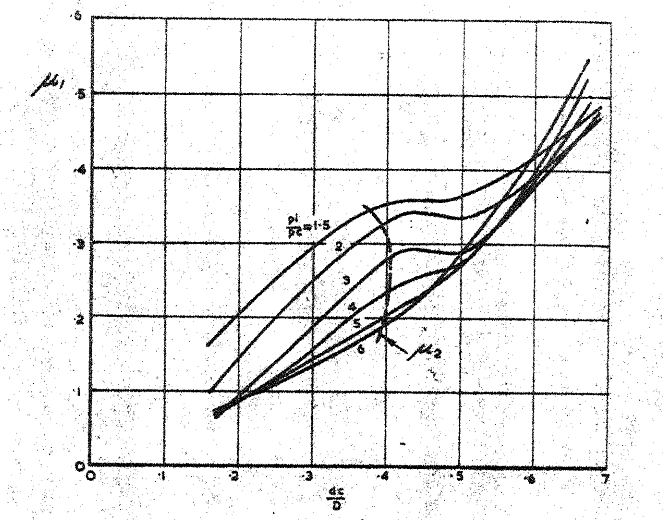

FIG. 55. VARIATION OF COLD MASS FLOW RATIO WITH COLD OUTLET DIAMETER RATIO AT OPTIMUM VALVE SETTING $\frac{d_i}{D} = .376$

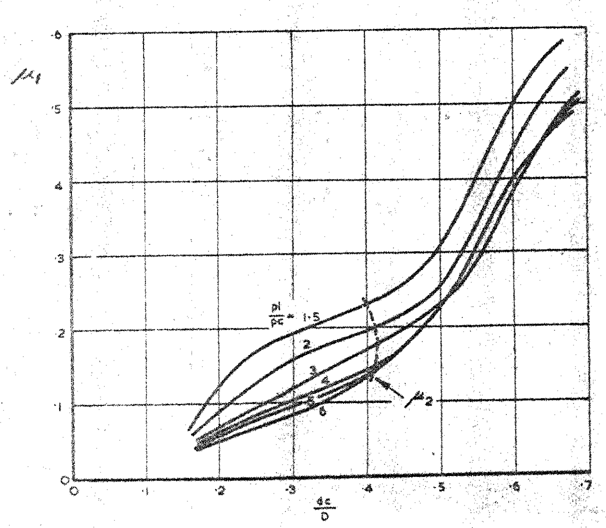

FIG. 56. VARIATION OF COLD MASS FLOW RATIO WITH COLD OUTLET DIAMETER RATIO AT OPTIMUM VALVE SETTING $\frac{d_i}{D} = .461$

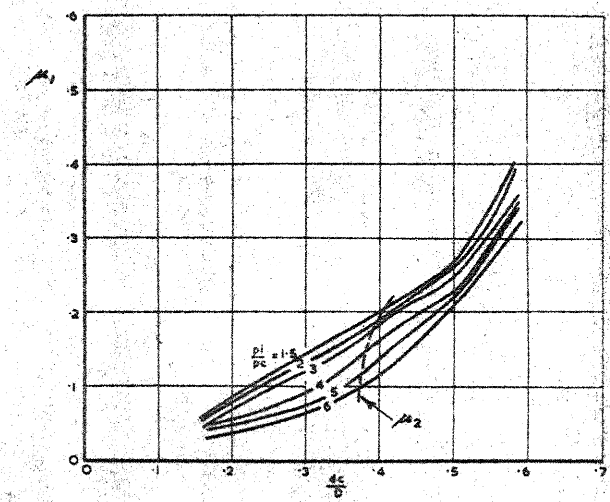

FIG. 57. VARIATION OF COLD MASS FLOW RATIO WITH COLD OUTLET DIAMETER RATIO AT OPTIMUM VALVE SETTING $\frac{d_i}{D} = .532$

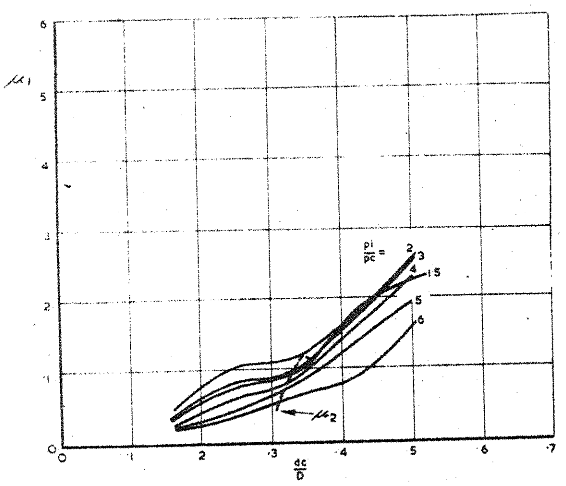

FIG. 58. VARIATION OF COLD MASS FLOW RATIO WITH COLD OUTLET DIAMETER RATIO AT OPTIMUM VALVE SETTING $\frac{d_i}{D}$ = .595

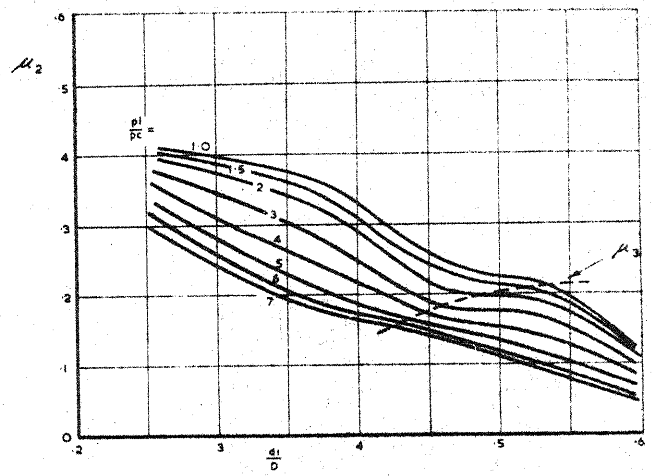

FIG. 59. VARIATION OF COLD MASS FLOW RATIO WITH INLET DIAMETER RATIO AT OPTIMUM VALVE SETTING AND OPTIMUM COLD OUTLET DIAMETER.

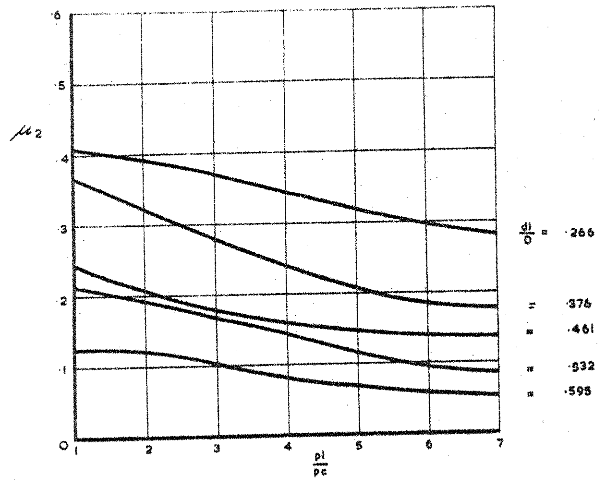

FIG. 60. VARIATION OF COLD MASS FLOW RATIO WITH PRESSURE RATIO AT OPTIMUM VALVE SETTING AND OPTIMUM COLD OUTLET DIAMETER.

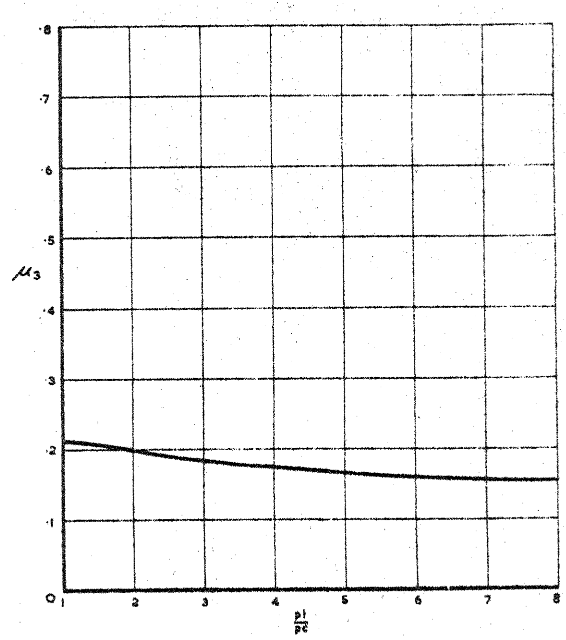

FIG. 61. VARIATION OF COLD MASS FLOW RATIO WITH PRESSURE RATIO FOR OPTIMUM VALVE SETTING, OPTIMUM COLD OUTLET DIAMETER RATIO AND OPTIMUM INLET DIAMETER

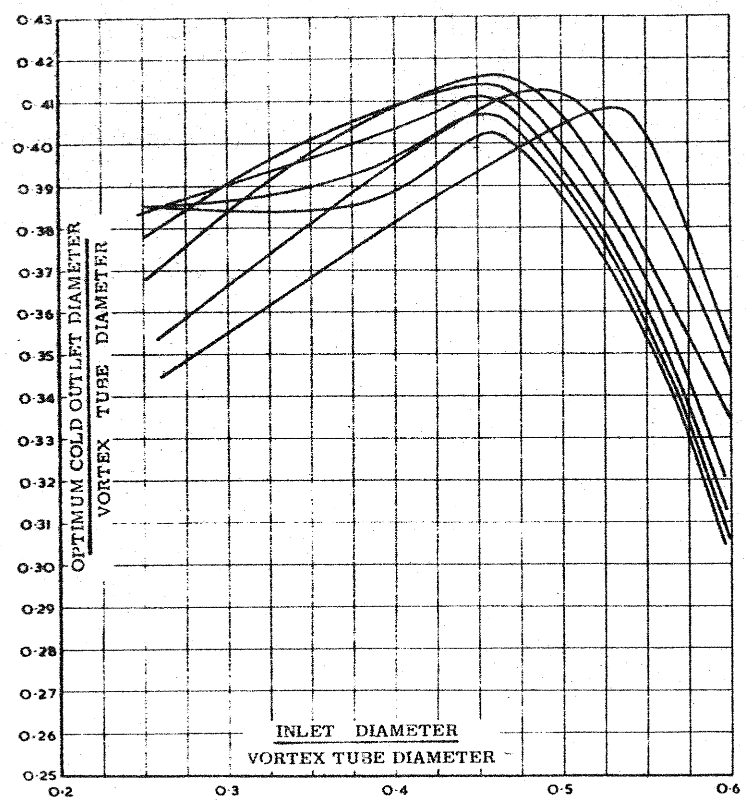

FIG. 62. VARIATION OF OPTIMUM COLD OUTLET DIAMETER WITH INLET DIAMETER

$\frac{p_i}{p_c}$ = 1.5, 2, 3, 4, 5, 6 and 7

$$\left(\frac{d_c}{D}\right)_1 \sim \frac{d_i}{D}$$

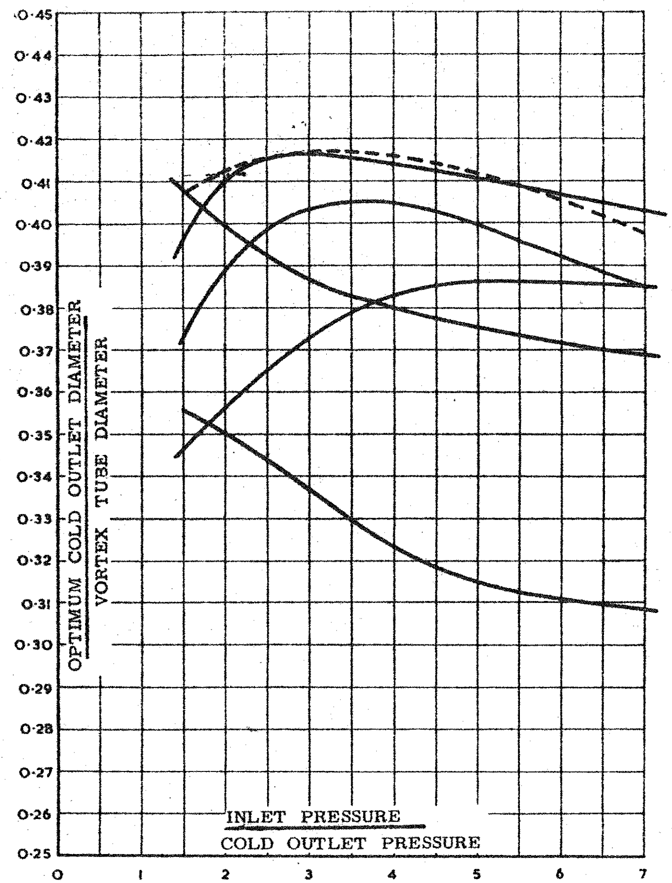

FIG. 63. VARIATION OF OPTIMUM COLD OUTLET DIAMETER WITH PRESSURE RATIO FOR FIXED INLET DIAMETERS, $\frac{d_i}{D}$ = .266, .376, .461, .532 & .595

$$\left(\frac{d_c}{D}\right)_1 \sim \frac{p_i}{p_c}$$

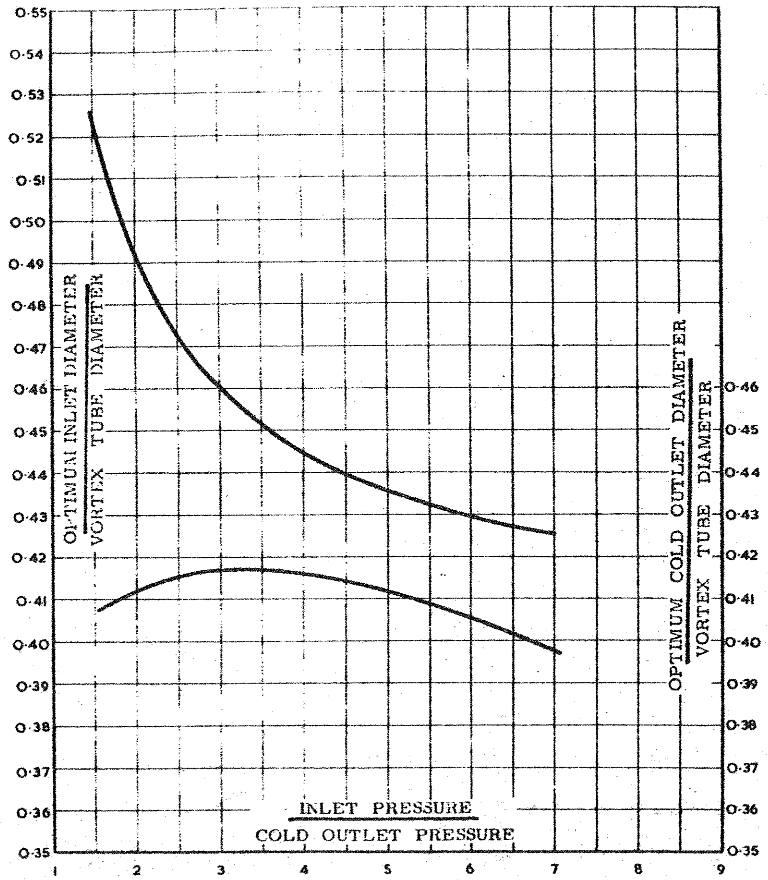

FIG. 64 OPTIMUM INLET AND COLD OUTLET DIAMETERS FOR FOR MAXIMUM TEMPERATURE DROP

$$\left(\frac{d_i}{D}\right)_1 \sim \frac{p_i}{p_c}$$

$$\left(\frac{d_c}{D}\right)_2 \sim \frac{p_i}{p_c}$$

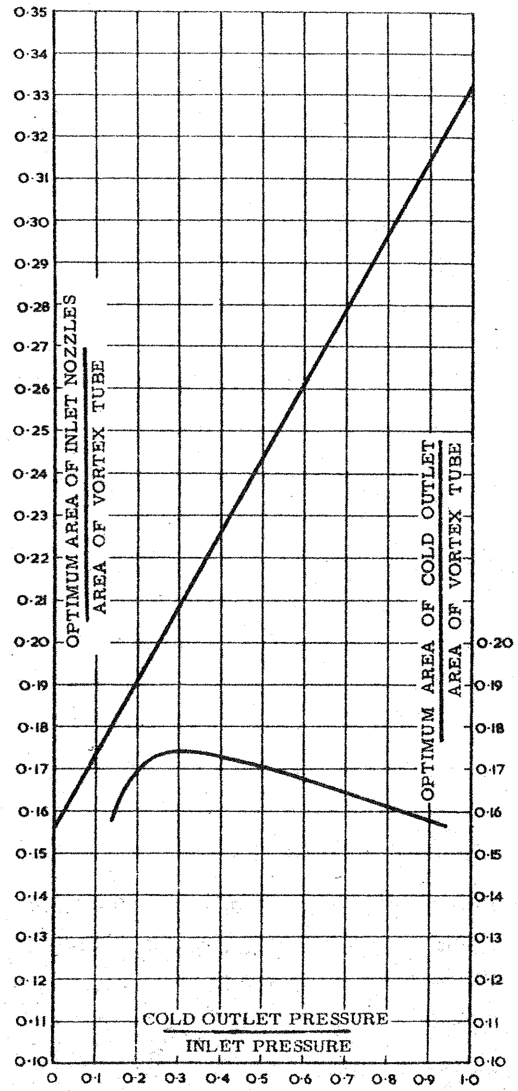

FIG. 65. OPTIMUM INLET AND COLD OUTLET AREAS FOR MAXIMUM TEMPERATURE DROP.

$$\left(\frac{A_i}{A}\right)_1 \sim \frac{p_i}{p_c}$$

$$\left(\frac{A_c}{A}\right)_2 \sim \frac{p_i}{p_c}$$